


Baterías de Litio



Porqué Li?



Periodic Table of Elements

1	2											3	4	5	6	7	8	9	10
H	He											Li	Be	B	C	N	O	F	Ne
3	4	5	6	7	8	9	10	11	12	13	14	15	16	17	18	19	20		
Na	Mg	Al	Si	P	S	Cl	Ar	K	Ca	Sc	Ti	V	Cr	Mn	Fe	Co	Ni		
37	38	39	40	41	42	43	44	45	46	47	48	49	50	51	52	53	54		
Rb	Sr	Y	Zr	Nb	Mo	Tc	Ru	Rh	Pd	Ag	Cd	In	Sn	Sb	Te	I	Xe		
55	56	57	72	73	74	75	76	77	78	79	80	81	82	83	84	85	86		
Cs	Ba	*La	Hf	Ta	W	Re	Os	Ir	Pt	Au	Hg	Tl	Pb	Bi	Po	At	Rn		
87	88	89	104	105	106	107	108	109	110	111	112	113	114	115	116	117	118		
Fr	Ra	+Ac	Rf	Ha	106	107	108	109	110	111	112	113	114	115	116	117	118		

* Lanthanide Series

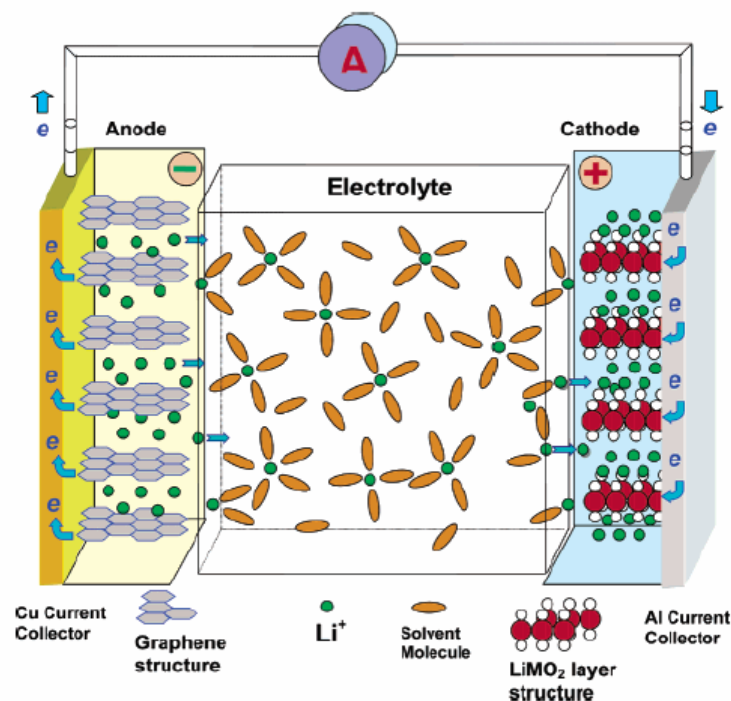
58	59	60	61	62	63	64	65	66	67	68	69	70	71
Ce	Pr	Nd	Pm	Sm	Eu	Gd	Tb	Dy	Ho	Er	Tm	Yb	Lu

+ Actinide Series

90	91	92	93	94	95	96	97	98	99	100	101	102	103
Th	Pa	U	Np	Pu	Am	Cm	Bk	Cf	Es	Fm	Md	No	Lr

Legend - click to find out more...

- H - gas
- Li - solid
- Br - liquid
- Tc - synthetic
- Non-Metals
- Transition Metals
- Rare Earth Metals
- Halogens
- Alkali Metals
- Alkali Earth Metals
- Other Metals
- Inert Elements

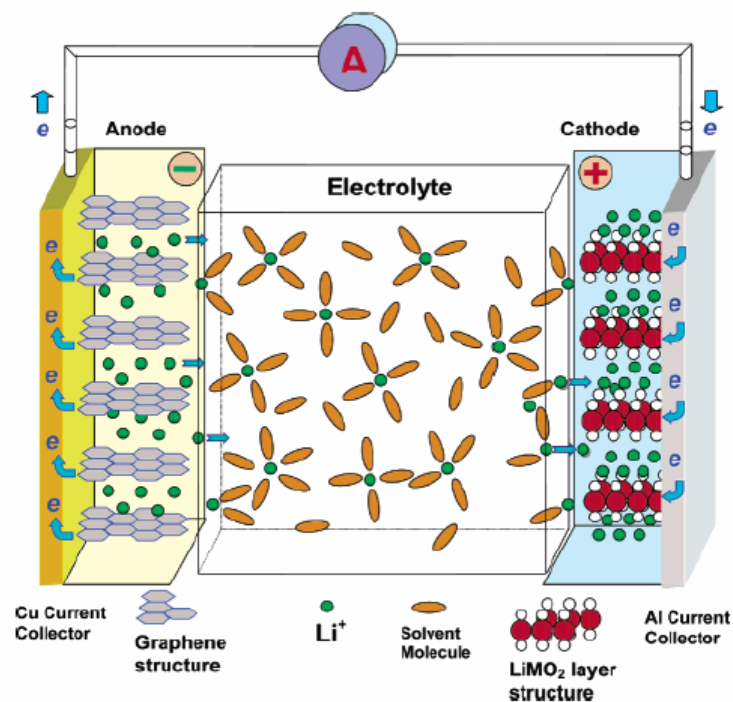




Porqué Li?

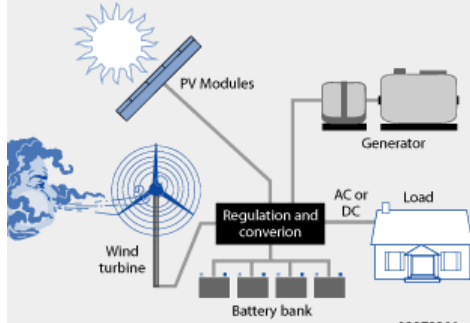


Li
N.A. 3
P.A. 6,939
Densidad $0,53 \text{ g cm}^{-3}$
Capacidad 3,88 A.h/g
Potencial -3,05 V vs. ENH



Hybrid Power Systems

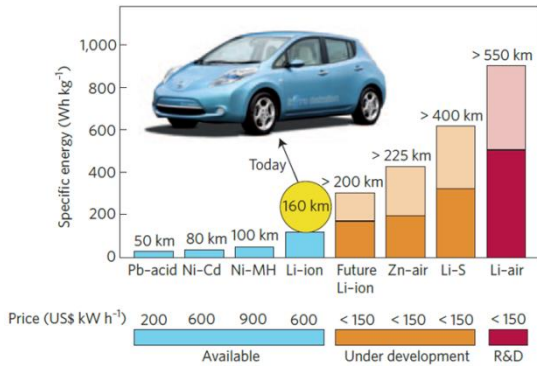
Combine multiple sources to deliver non-intermittent electric power



Remote Electrification (7.5 GWh market in South America)

Portable Electronics

Why is Lithium strategic for Energy Storage?



Electric Vehicles



Li-ion battery market 2016 87 GWh

PORTABLE ELECTRONICS (1990's-2010's)

Mobile Phones

Smart Phones (iphone)

Tablets

Increasing battery capacity (saturated market)

ELECTRIC VEHICLES (Emission Targets)

Hybrid

Plug.-in

Full electric (XEVs) (Tesla)- Electric Bus

China

2012 7% Li-ion batteries

2014 27% “

2016 50% “

2026 1 TWh (1000 GWh)

Source: Roskill Report

We observe an accelerated move to **low-carbon transport**



Volkswagen announces that it will roll out 80 new electric cars across its multi-brand group by 2025, up from a previous goal of 30, and wants to offer an electric version of each of its 300 group models by 2030. (12 Sept 2017)



BMW plans 25 all-electric and hybrid vehicles by 2025. (7 Sept 2017)



Honda will offer an electrified version of all of its new models launched in Europe from now on. (12 Sept 2017)



Honda, Toyota and Shell have teamed up to introduce more hydrogen refueling stations in California. (13 Sept 2017)



Hyundai has announced plans to rapidly roll out new all-electric models as the giant Korean car maker looks to explore new tech in the pursuit of more stable profits. (18 Aug 2017)



Volvo has announced that every Volvo it launches from 2019 will have an electric motor, marking the historic end of cars that only have an internal combustion engine (ICE) and placing electrification at the core of its future business. (5 June 2017)



The governments of **France and the U.K.** will ban sales of diesel and gasoline fueled automobiles by 2040. (July 2017)



China has announced that it will require all car manufacturers to have EV sales of 12% of total sales by 2020, and is planning to ban the sale of internal combustion engine powered cars by date that is to be decided. (June 2017, Sept 2017)

25,000 cars in the quarter january-march. 2017 500.000 in 2018

Lithium Batteries for Electric Car

450 kg battery 400 V cc. 60/75/90 kW (156 Wh/kg)
7104 cellx x 2,4 V = 17.050 Ah
4,453 g Li

Lithium Battery for a cell phone

4.9 Wh
1.32 mAh
0.344 g

With the mass of lithium in 1 car we can store the energy of 17.000 cell phones



GIGAFACTORY TESLA

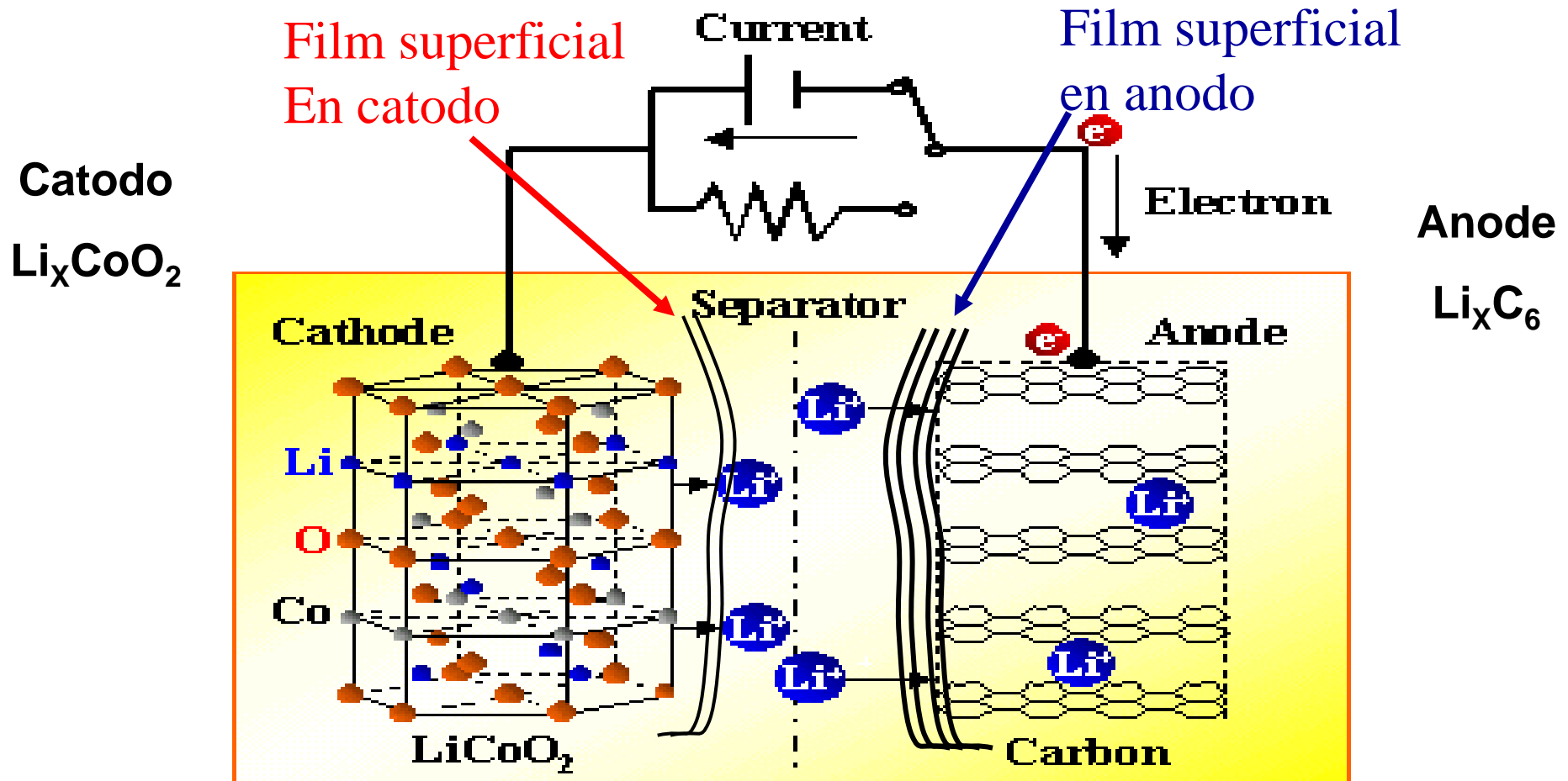
Electric Avenue. Sparks, NV 89434, EEUU

Tesla plans to manufacture 500.000 electric cars in 2018 (aprox. 2.250 ton of litium)



Baterias de Ion Litio

Las baterías de ion Li^+ usan varios componentes

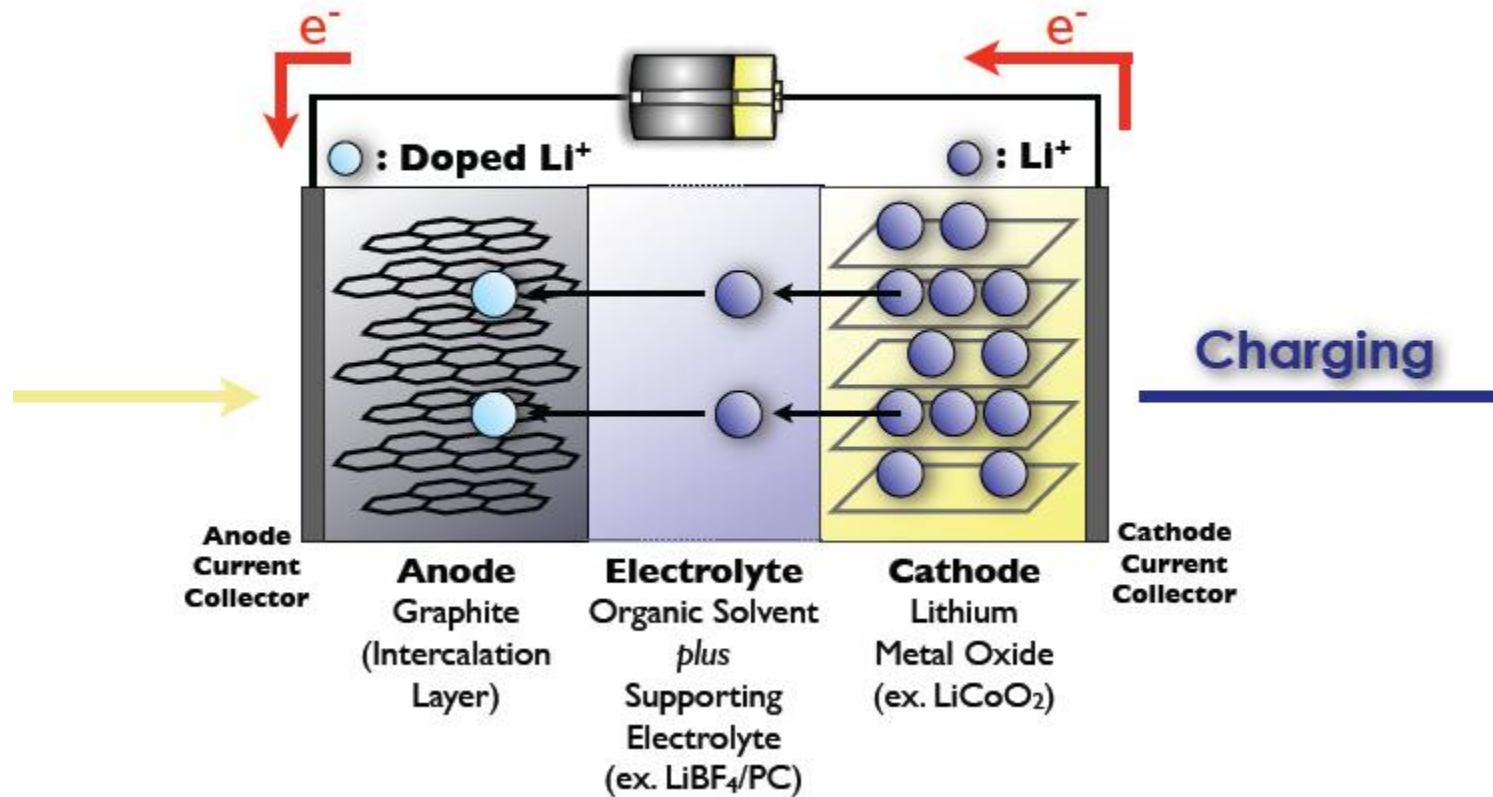


Soludion de Electrolito: **Carbonato de Etileno & Di-Metil Carbonato** / LiPF_6

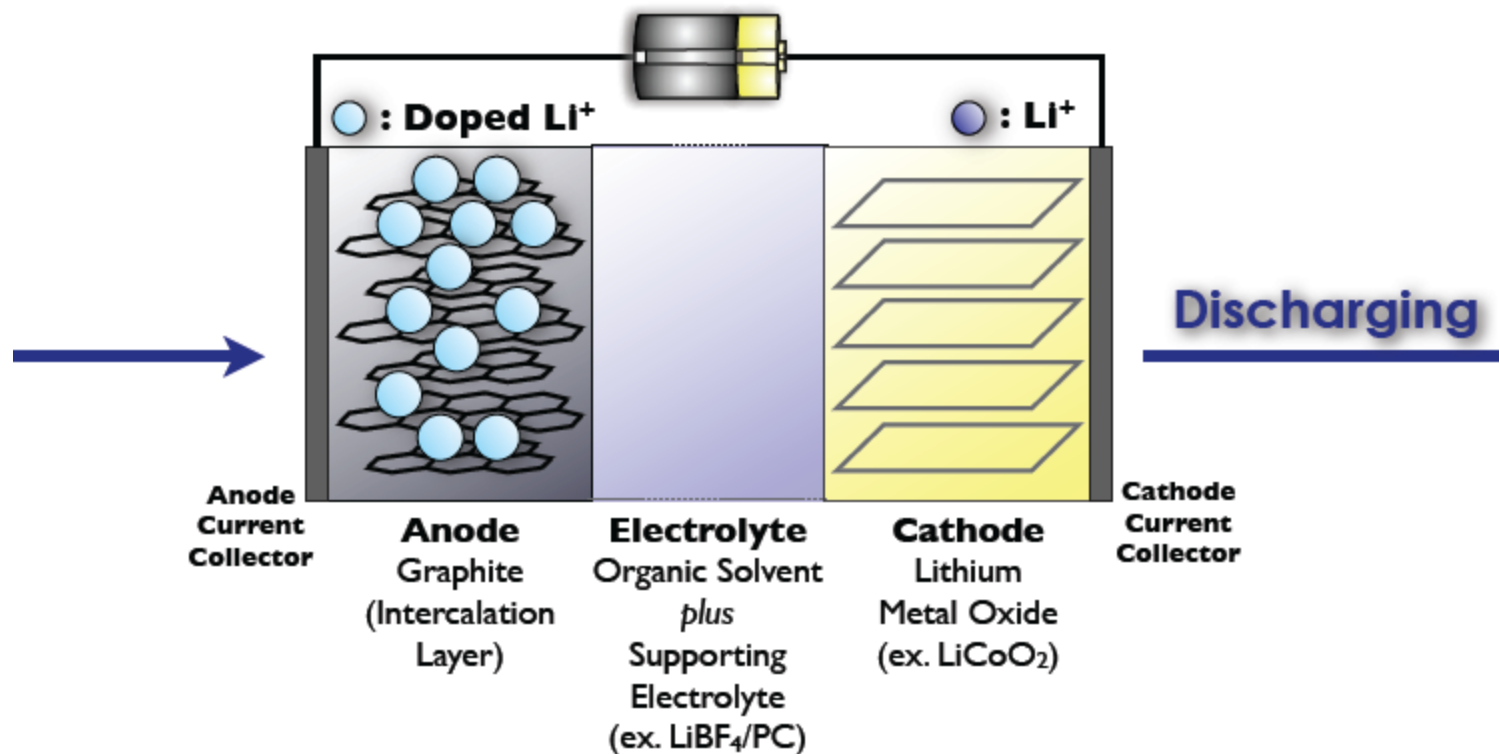
Voltage: 3.7 V, Densidad de Energia Media: 150 Wh/Kg

Mecanismo de Baterías de Li-ion

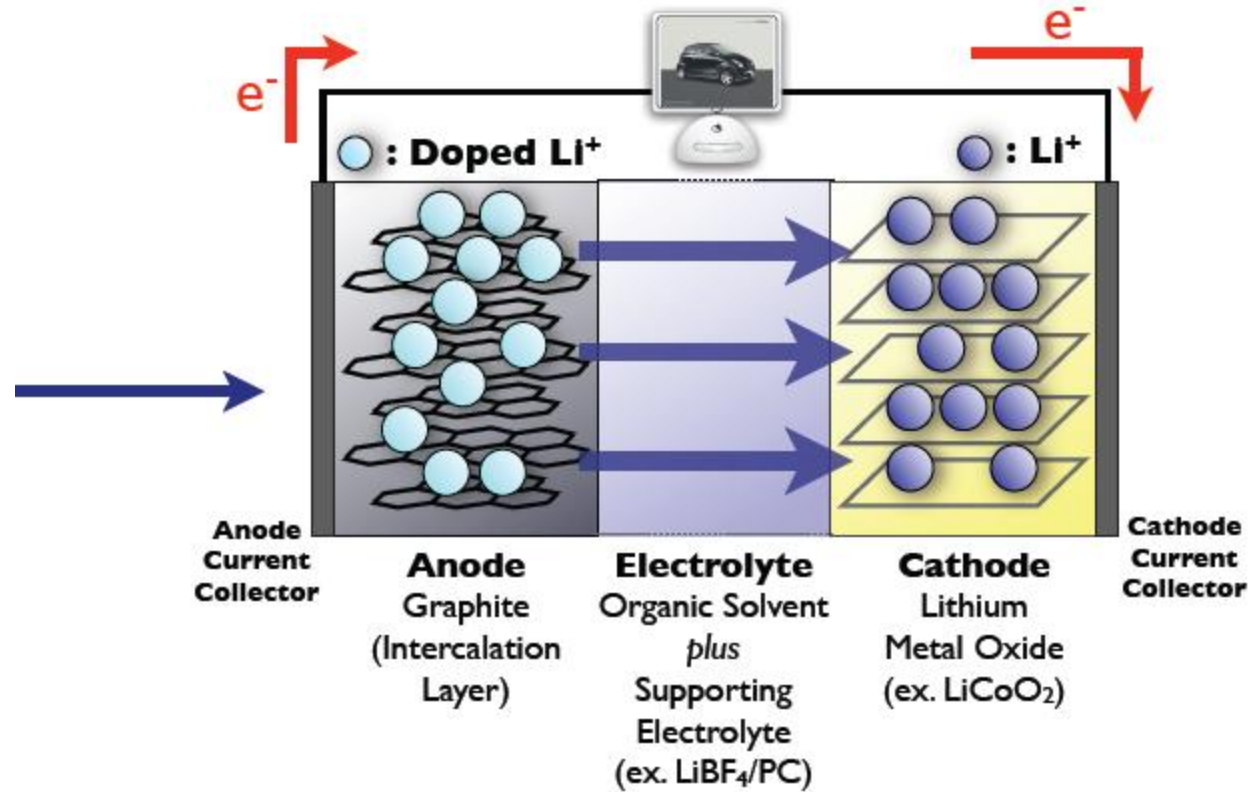
Sillón Hamaca (rocking chair)



Fully Charged State



Fully Discharged State

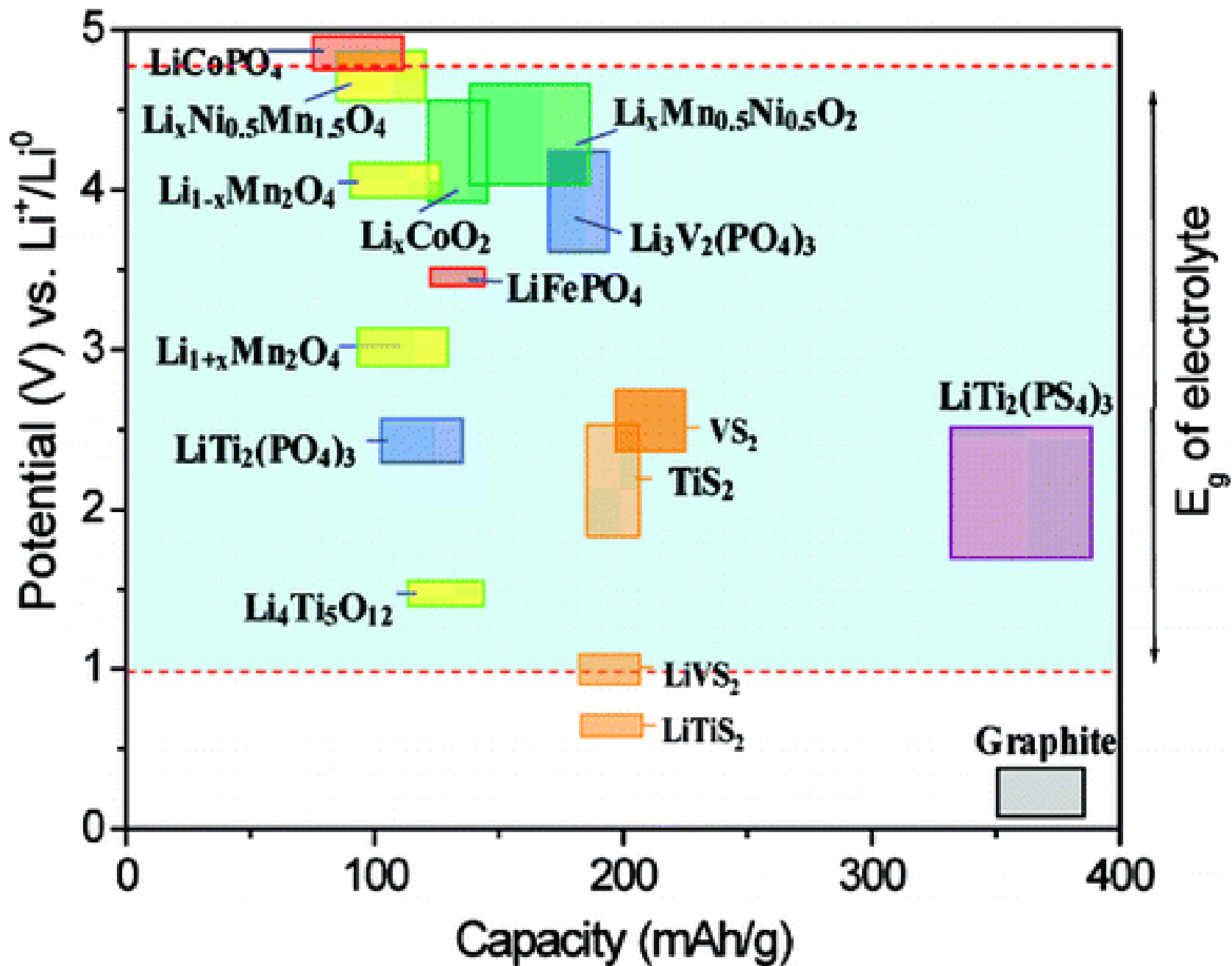


Anodo (-)

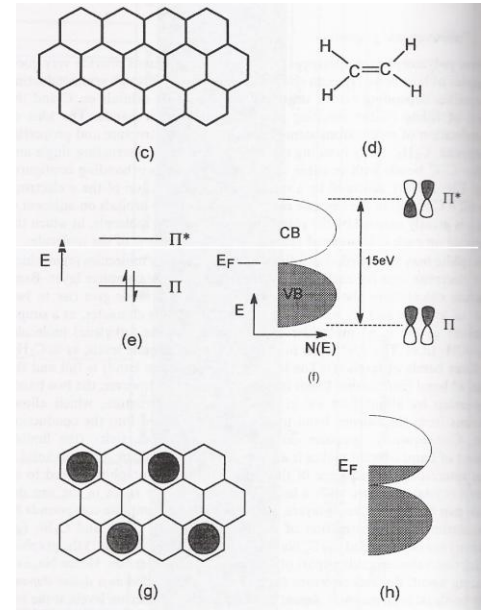
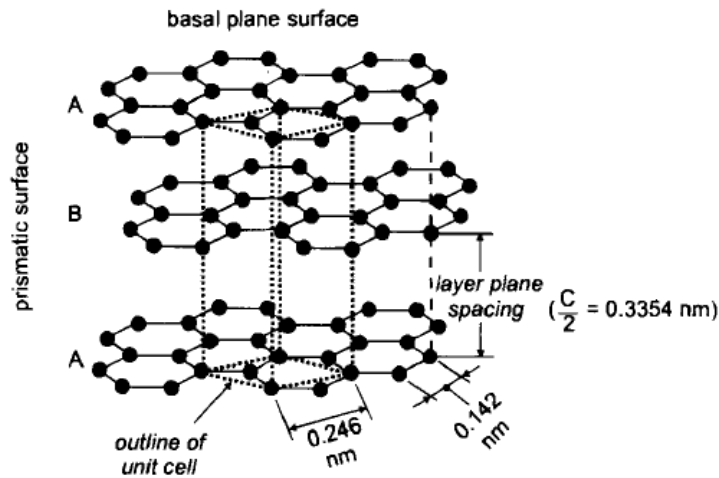
Electrode material	Average potential difference	Specific capacity	Specific energy
Graphite (LiC ₆)	0.1-0.2 V	372 mA·h/g	0.0372-0.0744 kW·h/kg
Hard Carbon (LiC ₆)	? V	? mA·h/g	? kW·h/kg
Titanate (Li ₄ Ti ₅ O ₁₂)	1-2 V	160 mA·h/g	0.16-0.32 kW·h/kg
Si (Li _{4.4} Si) ^[28]	0.5-1 V	4212 mA·h/g	2.106-4.212 kW·h/kg
Ge (Li _{4.4} Ge) ^[29]	0.7-1.2 V	1624 mA·h/g	1.137-1.949 kW·h/kg

Catodo (+)

Electrode material	Average potential difference	Specific capacity	Specific energy
LiCoO ₂	3.7 V	140 mA·h/g	0.518 kW·h/kg
LiMn ₂ O ₄	4.0 V	100 mA·h/g	0.400 kW·h/kg
LiNiO ₂	3.5 V	180 mA·h/g	0.630 kW·h/kg
LiFePO ₄	3.3 V	150 mA·h/g	0.495 kW·h/kg
Li ₂ FePO ₄ F	3.6 V	115 mA·h/g	0.414 kW·h/kg
LiCo _{1/3} Ni _{1/3} Mn _{1/3} O ₂	3.6 V	160 mA·h/g	0.576 kW·h/kg
Li(Li _a Ni _x Mn _y Co _z)O ₂	4.2 V	220 mA·h/g	0.920 kW·h/kg



Ánodo de Grafito



- graphite particles
- various SEI components
- Li-ions
- Cu foil

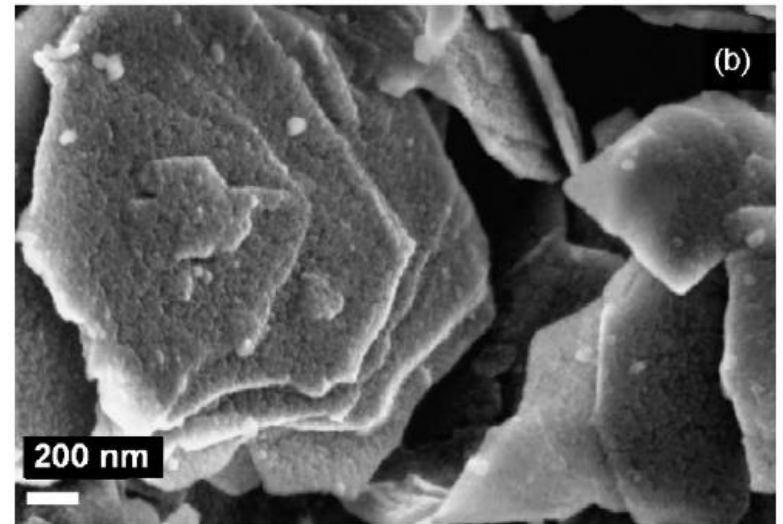
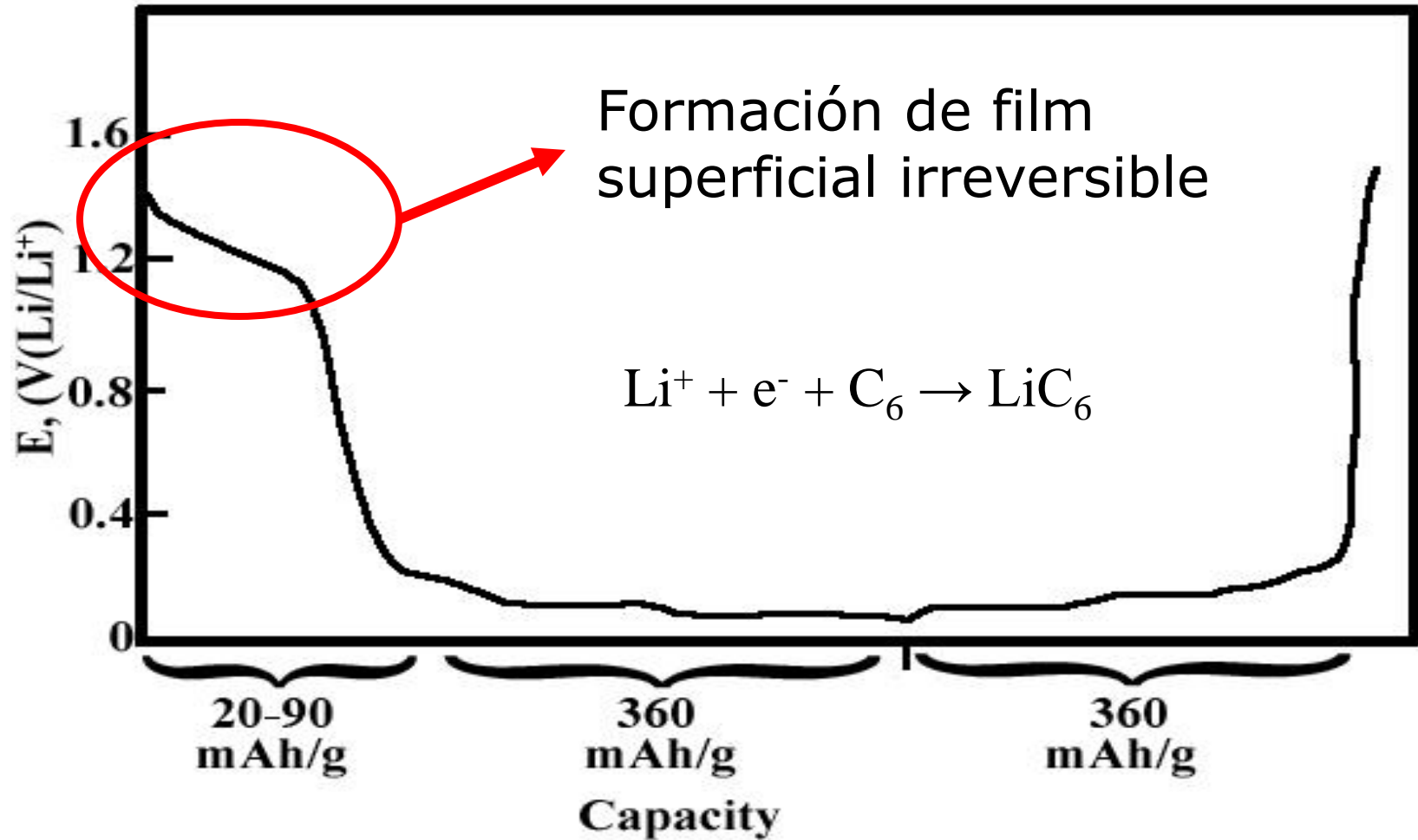


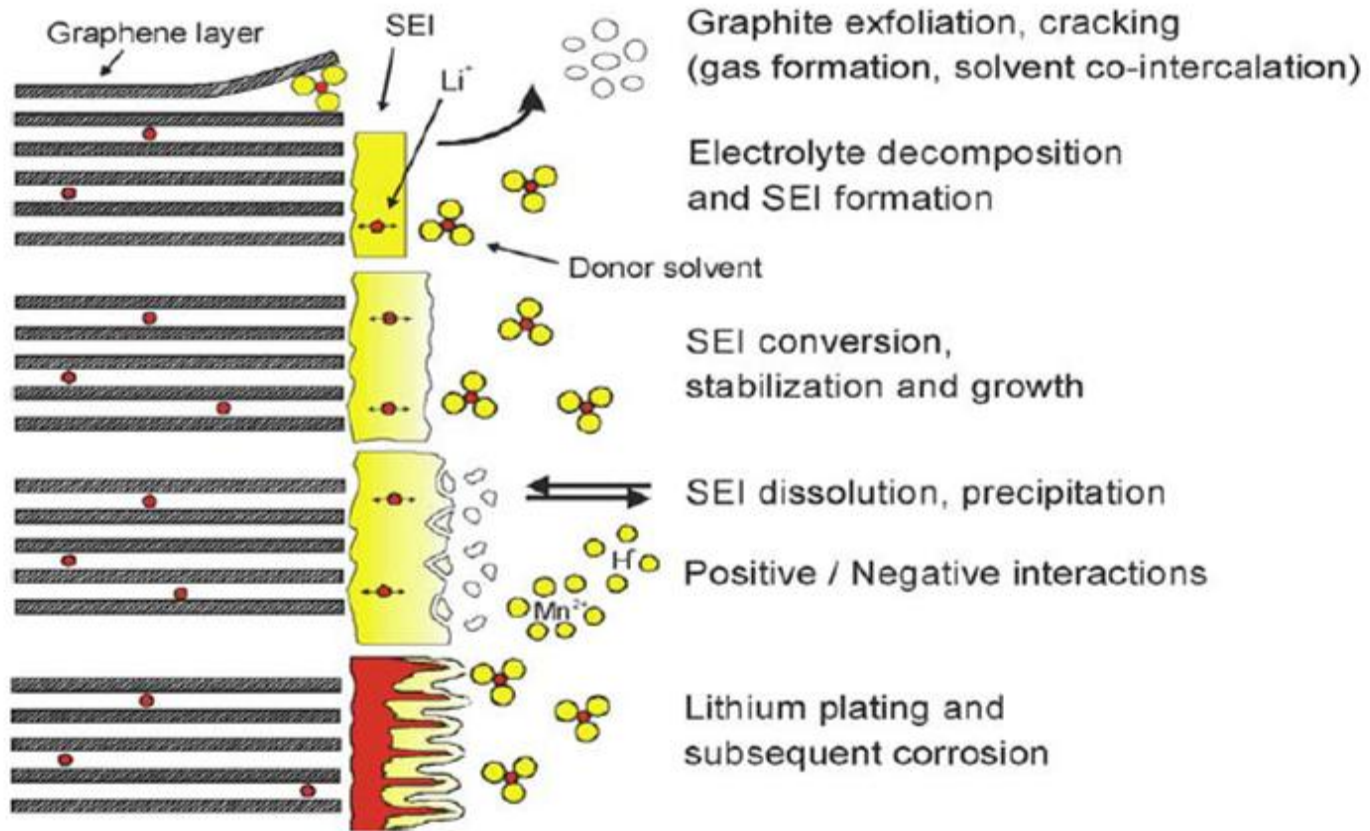
Fig. 3. SEM of composite SFG6 (TIMCAL[®]) graphite electrode (90% graphite and 10% PVDF-HFP binder): (a) pristine electrode and (b) electrode after one cycle vs. Li metal in 1 M LiPF₆ in EC:DMC (1:1) electrolyte at C/10 rate.

Perfil de Potencial

Primer Ciclo



Formacion de un film superficial, SEI



Changes at the anode/electrolyte interface, from *J. Vetter et al. / Journal of Power Sources 147 (2005) 269–281*

Cátodo de Inserción de ión Li^+

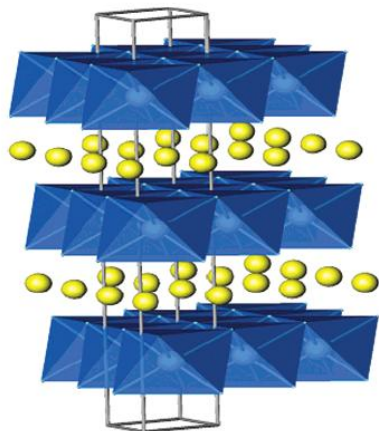


Figure 1. Layered structure of LiTiS_2 , LiVSe_2 , LiCoO_2 , LiNiO_2 , and $\text{LiNi}_x\text{Mn}_y\text{Co}_{1-2y}\text{O}_2$, showing the lithium ions between the transition-metal oxide/sulfide sheets. The actual stacking of the metal oxide sheets depends on the transition metal and the anion.

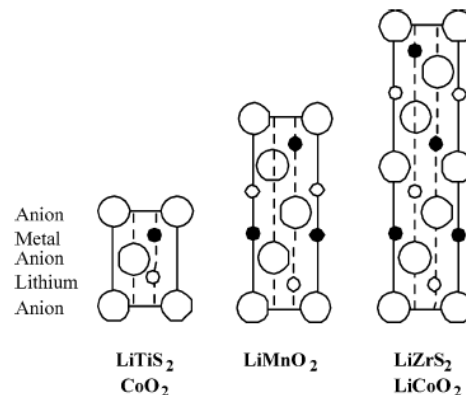
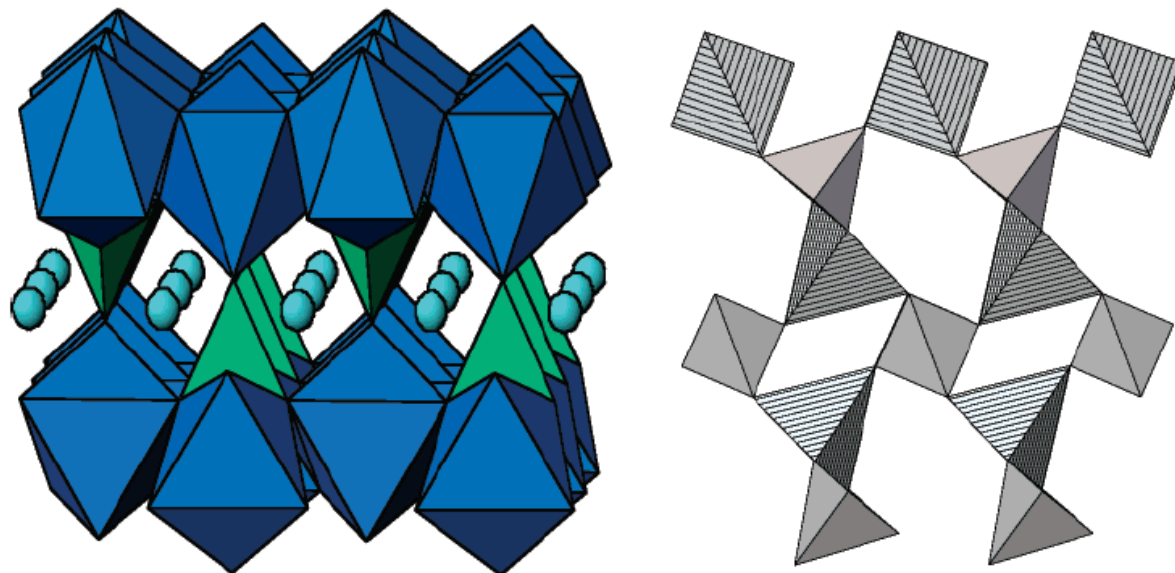


Figure 10. Schematic of stacking of building blocks for one-block, two-block, and three-block structures.



Structures of orthorhombic LiFePO_4 and trigonal quartz-like FePO_4 .

Separadores

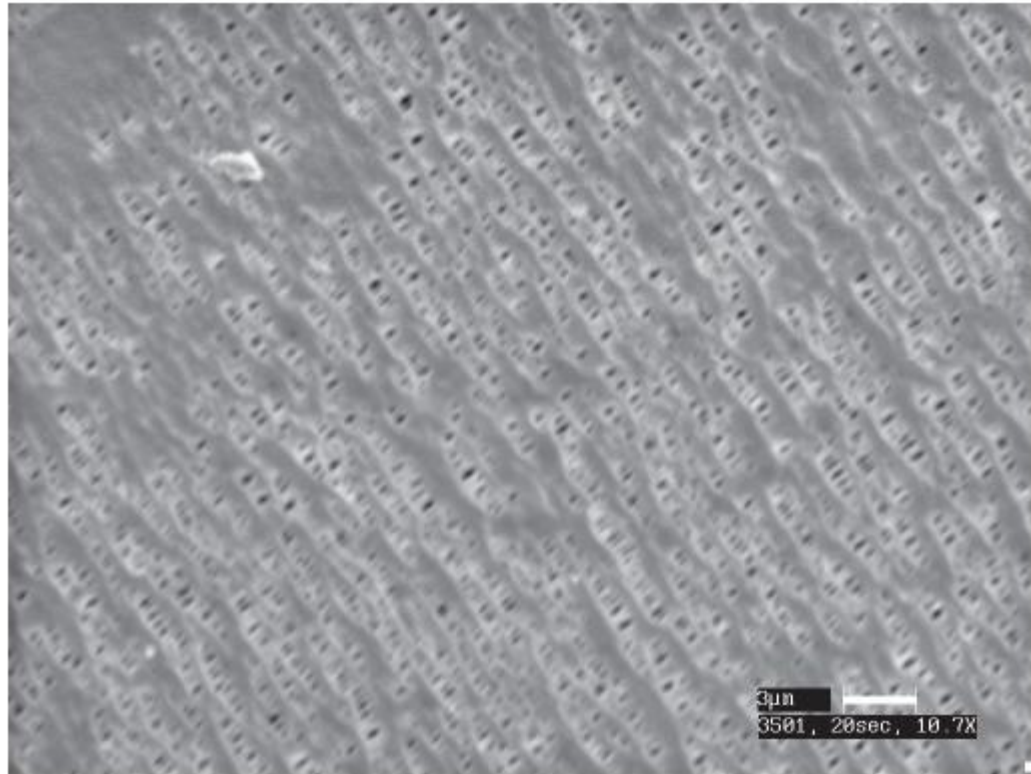


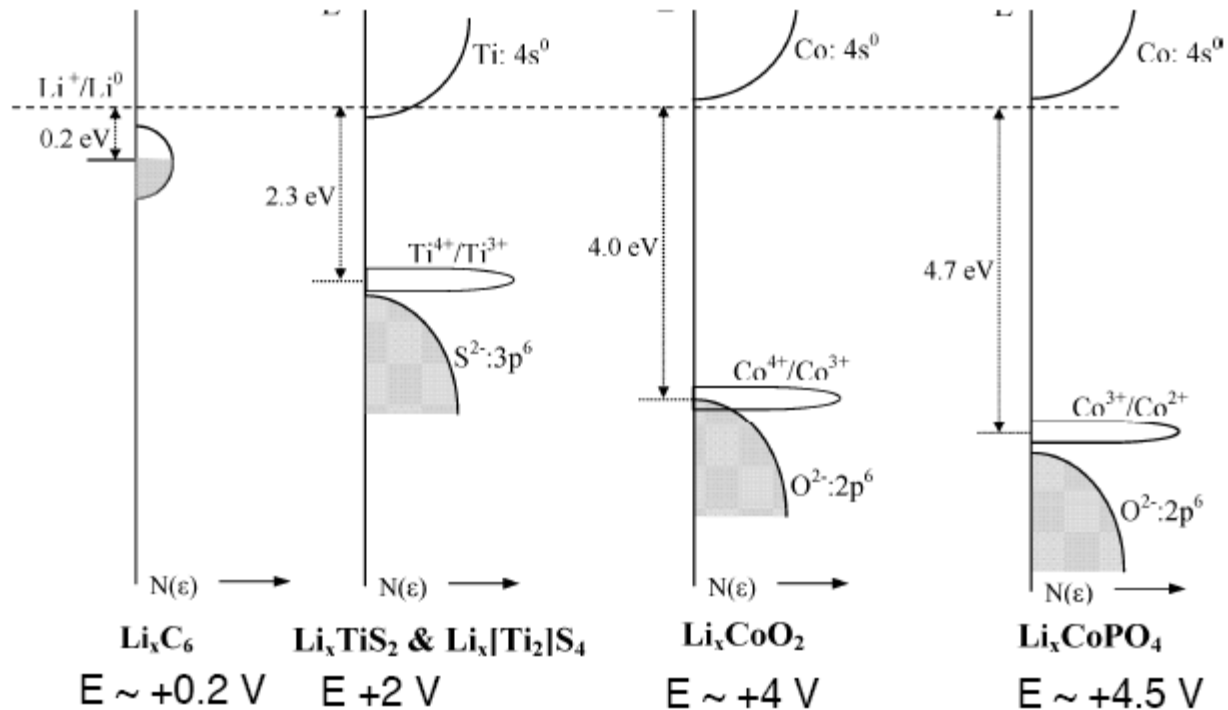
FIGURE 35.28 SEM micrograph of Celgard 3501 separator. (*Courtesy of Yardney Technical Products, Inc.*)

What determines the electrode potential?

$$E = -\mu_{\text{Li}}/F = -(\mu_{\text{Li}^+} + \mu_{\text{e}^-})/F$$

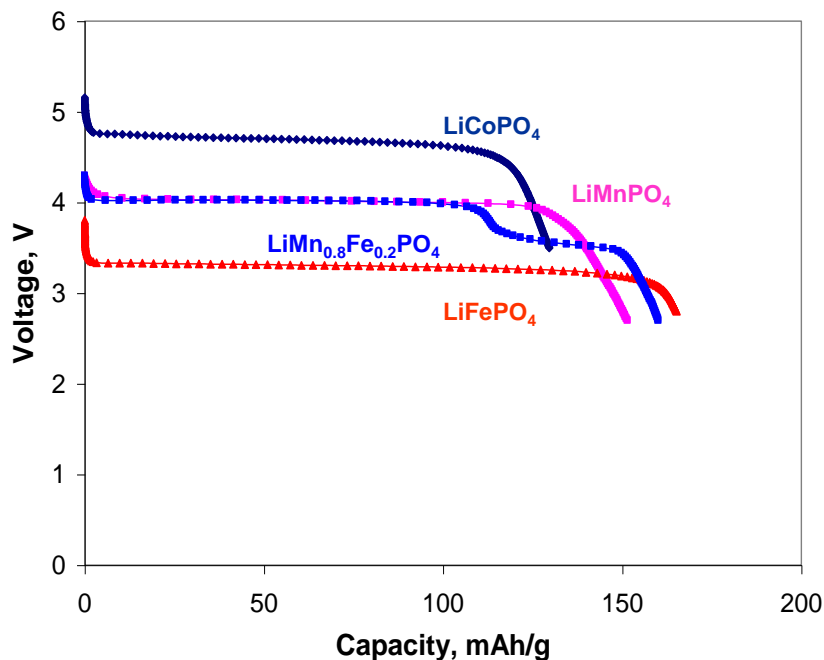
1. The ELECTRON ENERGY

The Fermi level is the chemical potential of the electron, μ_{e} (always -ve)



The LiMPO₄ Family: Optimization of Olivine Cathodes for Li-ion Batteries

Olivine	Voltage Range (V)	theoretical Energy Density (mAh/ g)
LiFePO ₄	3.4	170 (165 practical)
LiMnPO ₄	4.2	170 (150 practical)
LiMn _{0.8} Fe _{0.2} PO ₄	4.2	170 (160 practical)
LiCoPO ₄	4.8	170 (130-140 practical)



Advantages of olivine cathodes:

- High capacity
- Flat voltage profile

For LiFePO₄, LiMnPO₄, LiMn_{0.8}Fe_{0.2}PO₄:

- Low cost
- Low toxicity
- High rate capability

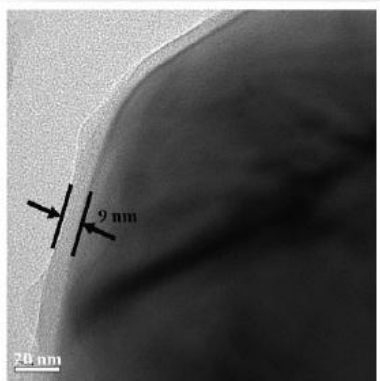
For LiCoPO₄

- High voltage

How to improve performance:

Electronic conductivity:

- Thin carbon coating
- Aliovalent dopants



Li-Ion Diffusion:

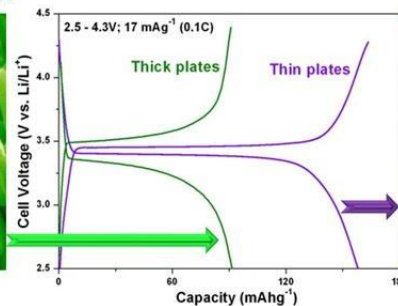
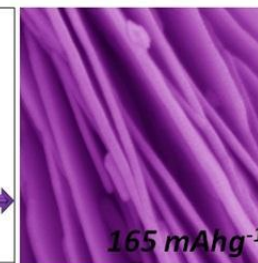
- Reduce particle size (nano particles)
- Aliovalent dopants
- Solid solution

* HR-TEM image of the $\text{LiFe}_{0.9}\text{Mg}_{0.1}\text{PO}_4/\text{C}$ sample

Thickness $100 \pm 5 \text{ nm}$

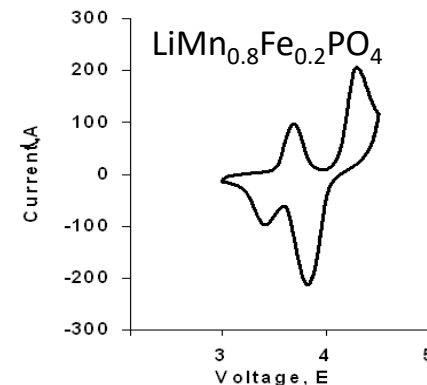
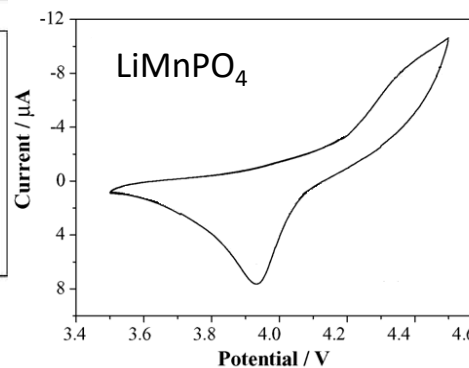
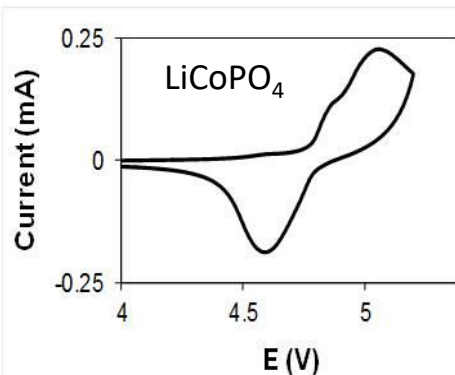
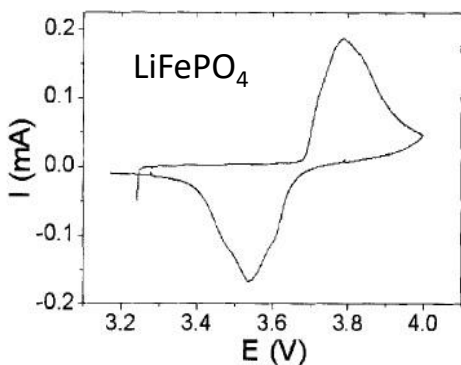


Thickness $30 \pm 5 \text{ nm}$



Comparison of LiFePO_4 nanoplates with thick plates [Saravanan et al. *J. Mater. Chem.*, 19 (2009) 605].

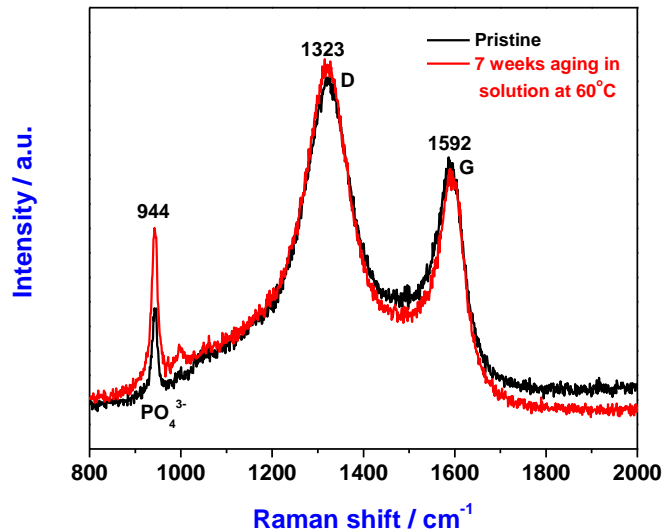
Cyclic voltammetry



* Hui Liua, Jingying Xie, *Journal of materials processing technology*, 209(2009)

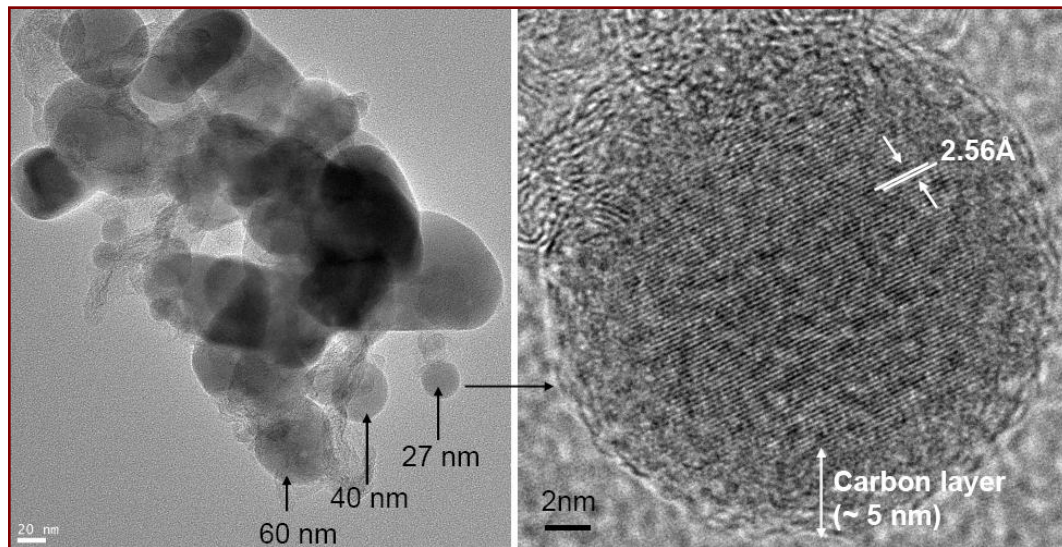
Impact of Aging in Solutions: Morphology of C-LiMn_{0.8}Fe_{0.2}PO₄: Highly Stable

Raman

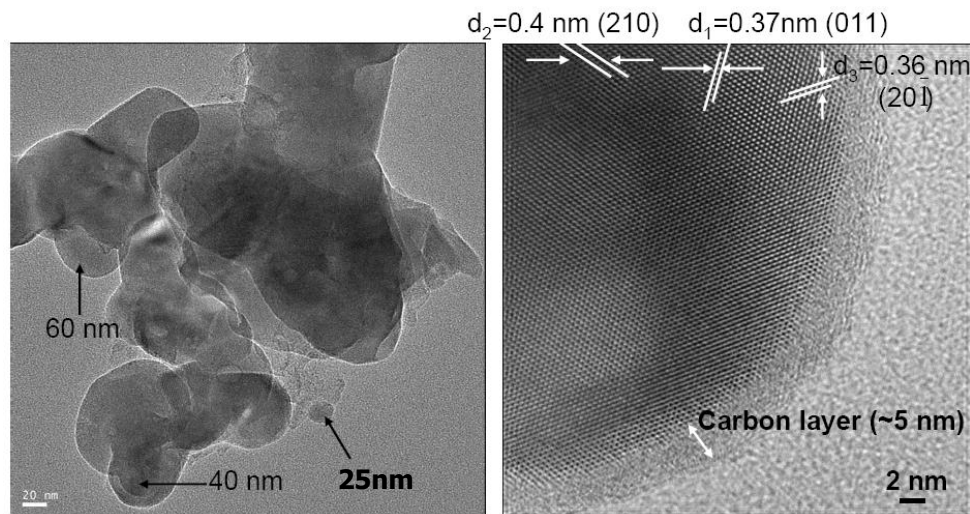


C-LiMn_{0.8}Fe_{0.2}PO₄ particles do not undergo any morphological changes upon prolonged aging at 60°C

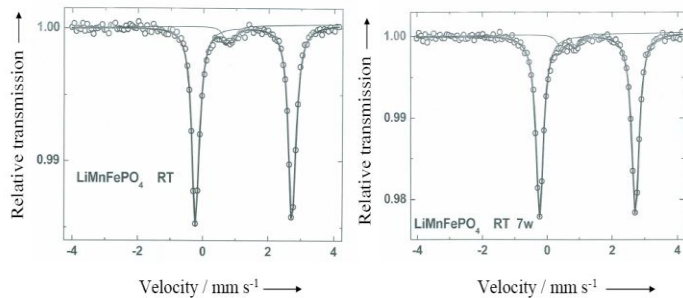
Pristine C-LiMn_{0.8}Fe_{0.2}PO₄



3 week aged at 60°C

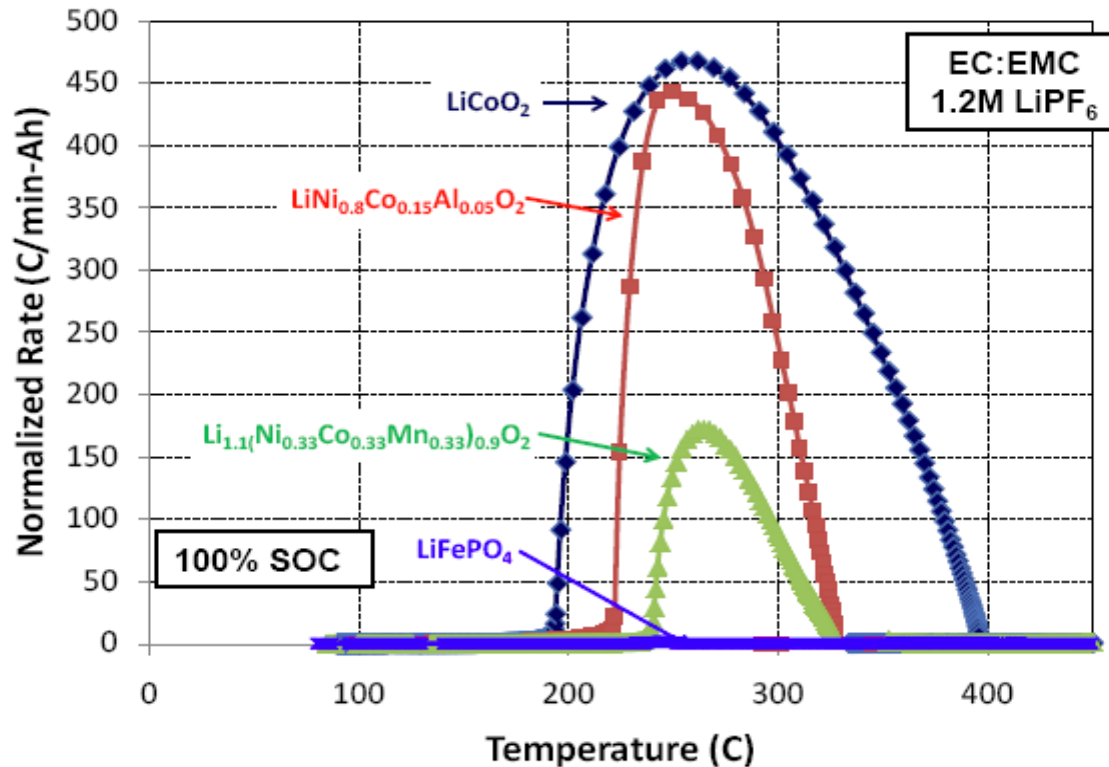


pristine Mossbauer (Fe) aged



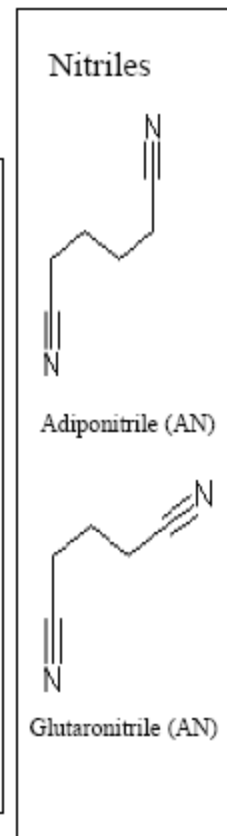
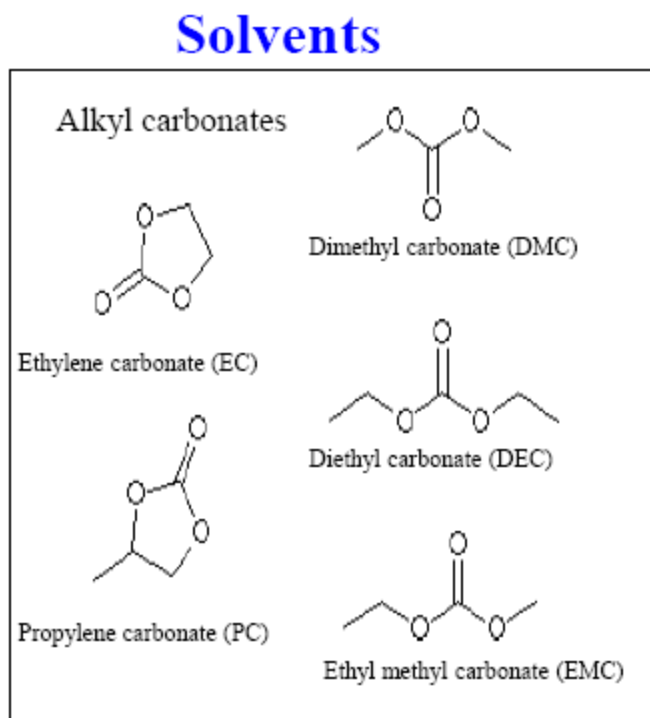
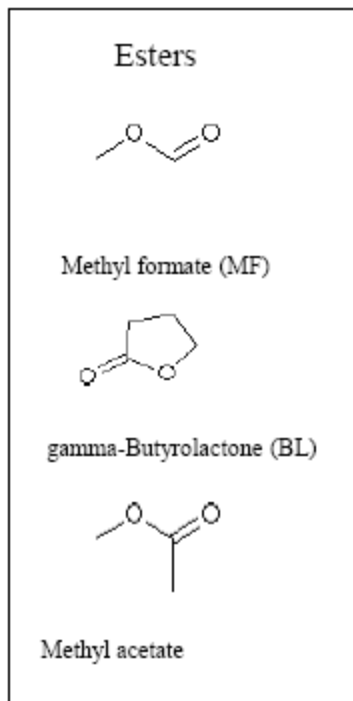
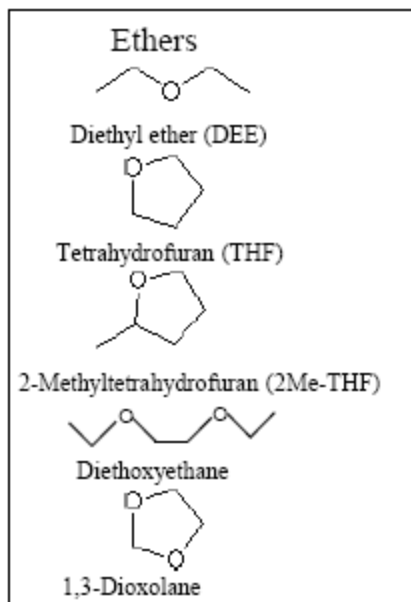
Thermal Runaway & Cathode Chemistry

Accelerating Rate Calorimetry (ARC)

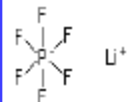
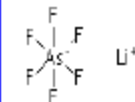
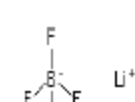
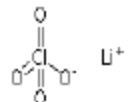
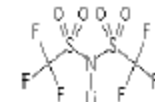
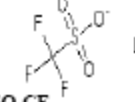
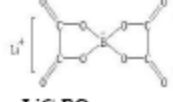
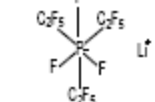


- Increased thermal runaway temperature and reduced peak heating rate for full cells
- Decreased cathode reactions associated with decreasing oxygen release

Electrolyte solutions for Li batteries



Relevant Li Salts

							
LiPF₆ Lithium hexafluorophosphate	LiAsF₆ Lithium hexafluoroarsenate	LiBF₄ Lithium tetrafluoroborate	LiClO₄ Lithium perchlorate	LiN(SO₂CF₃)₂ Lithium bis(trifluoromethane sulfonimide) (LiTFSI)	LiSO₃CF₃ Lithium trifluoromethane sulfonate (Lithium triflate)	LiC₂BO₄ Lithium bis(oxalate) borate (LiBOB)	LiPF₆(CF₃CF₃)₃ Lithium fluoroalkyl phosphate (LiFAP)

Baterias de litio-polímero

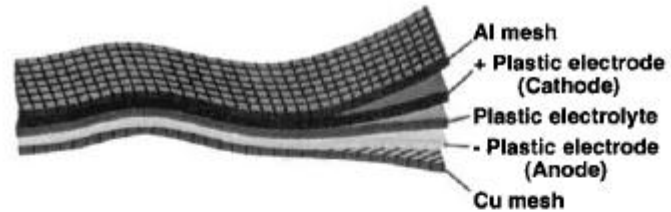


FIGURE 35.87 Schematic diagram showing the construction of a polymer Li-ion cell. (Courtesy of Telecordia.)



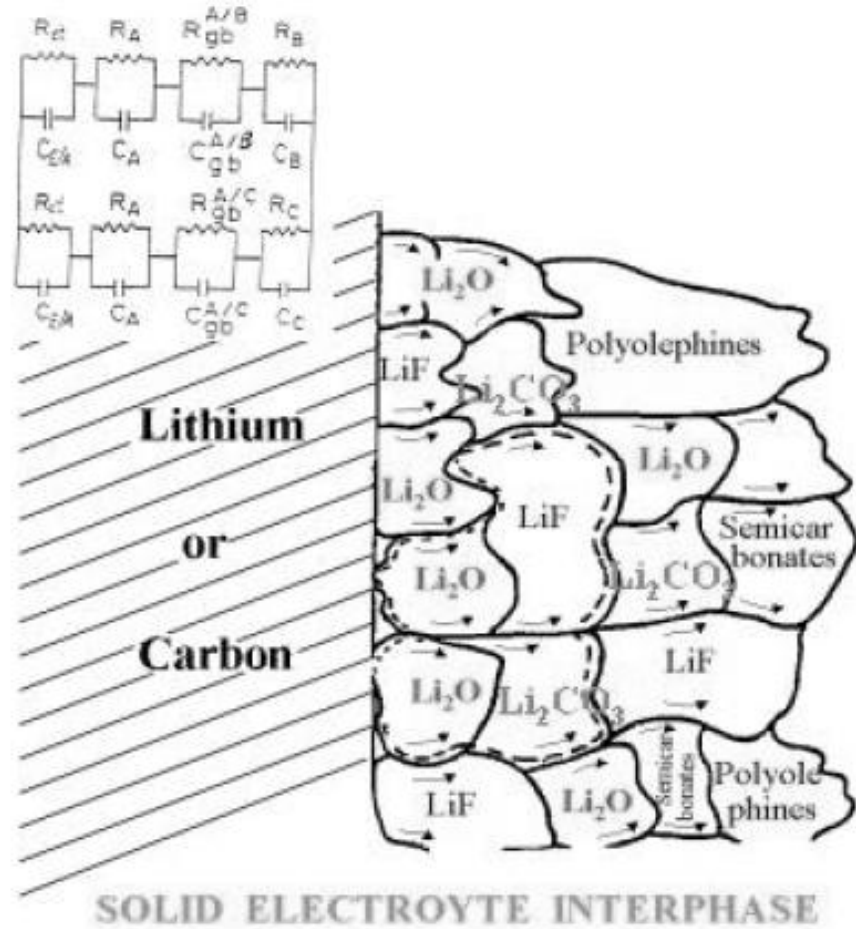
FIGURE 35.88 A 0.57 Ah polymer Li-ion battery. (Courtesy of Sanyo.)

DIFICULTADES

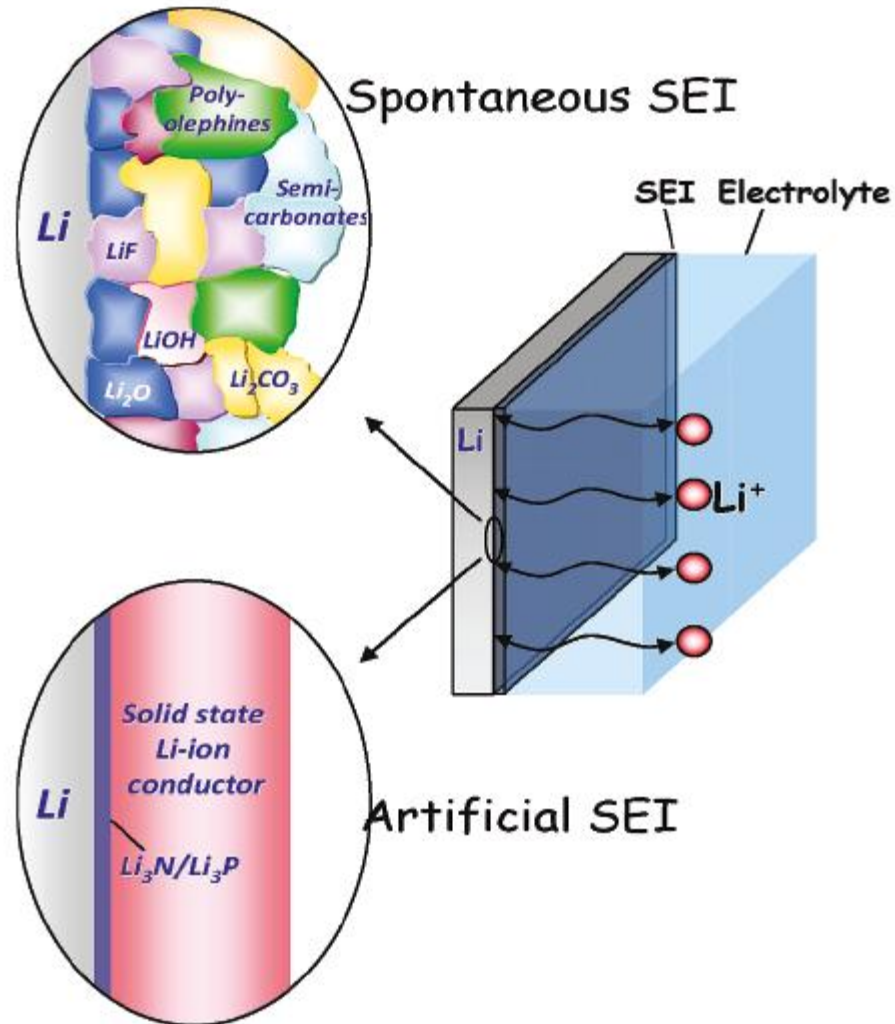
Las baterías son dispositivos muy complejos: 3 sólidos activos (ánodo, cátodo, electrolito) y dos interfaces electrodo-electrolito deben funcionar simultáneamente sin reacciones secundarias.

- **En baterías ion litio no hay estabilidad termodinámica**
- **En el ánodo, por debajo de 1 V vs. Li/Li⁺ la mayoría de los solventes, aniones de las sales pueden reducirse en particular en presencia de iones Li⁺.**
- * **En el cátodo: Todos los óxidos de metales de transición litados son nucleofílicos y básicos, pueden reaccionar con solventes electrofílicos.**
Ocurren reacciones ácido-base con HF y PF₅, intercambio de protones con iones metálicos y disolución.
- **En los cátodos de-litados podemos encontrar inestabilidad anódica de solvente y problemas con colectores de corriente.**
- **¿Qué colector de corriente usamos? La mayoría de los metales se disuelven a potenciales anódicos moderados. Los metales preciosos como Au y Pt son caros y catalíticos.**
- **Se eligió Al debido a su pasivación, pero la pasivación de Al no es estable más allá de ciertos umbrales de potencial entre 4-5 V**

SOLID ELECTROLYTE INTERPHASE (SEI)

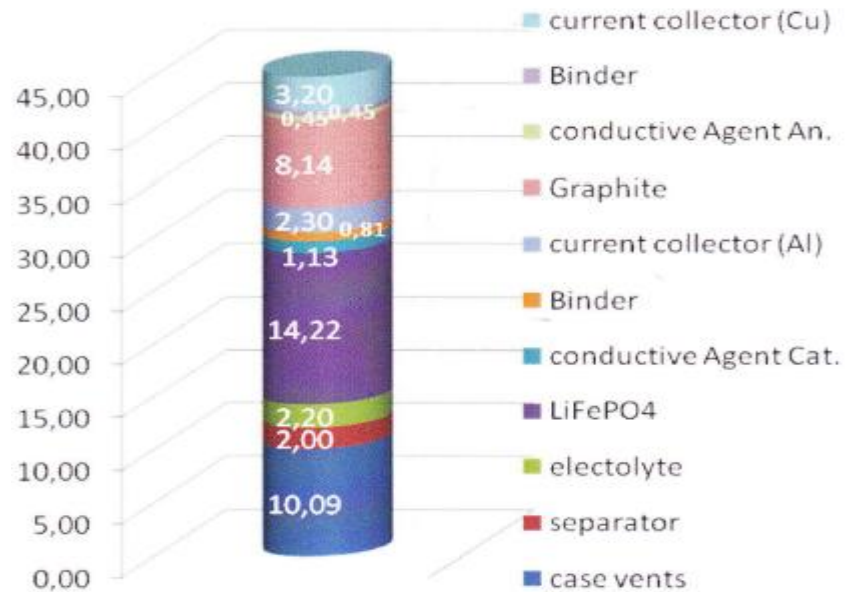
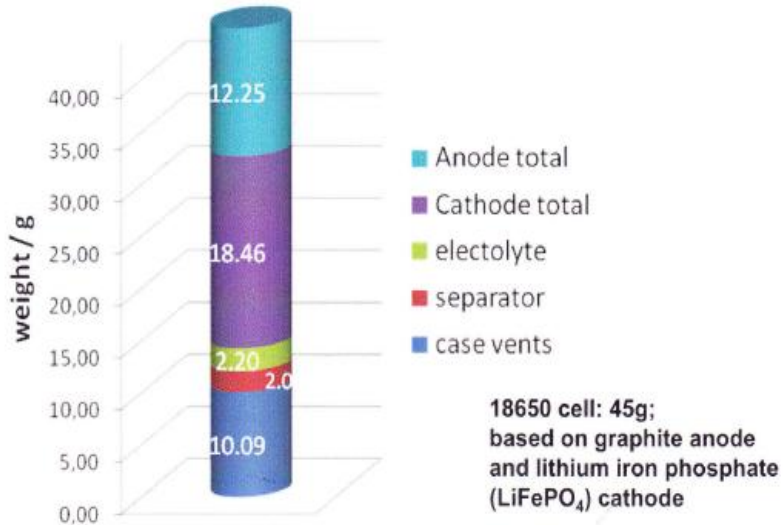
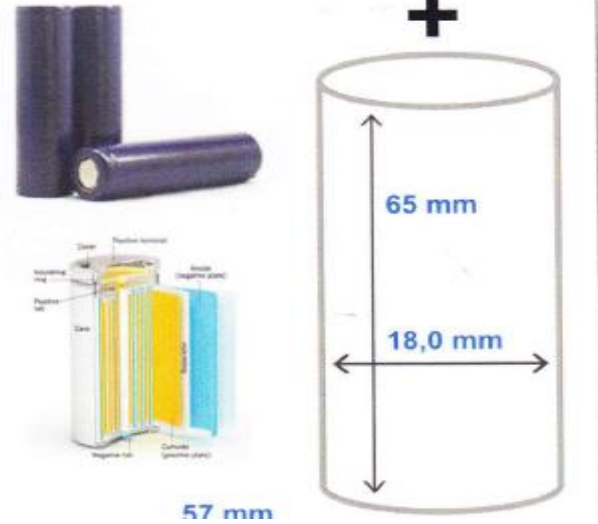
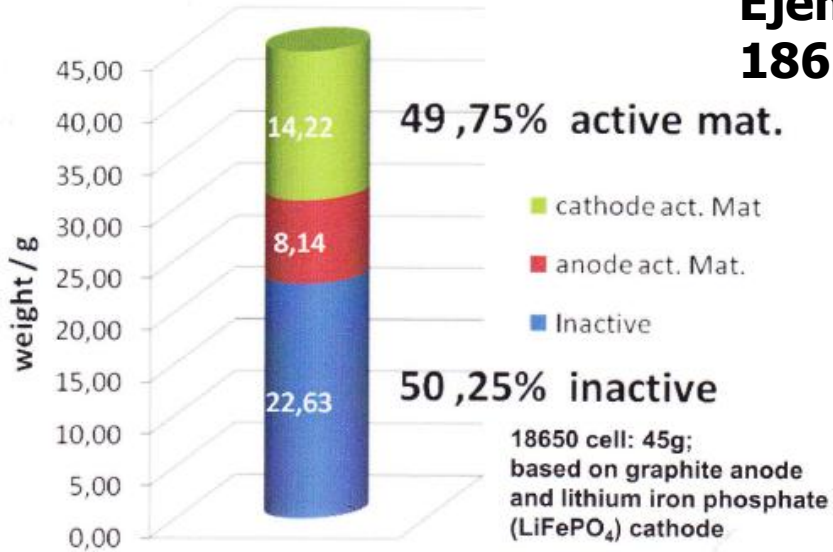


Interfaz Electrolyto Solido (SEI)



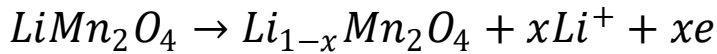
Baterias de ion litio comunes y su distribucion de masa

Ejemplo: 18650 celdas

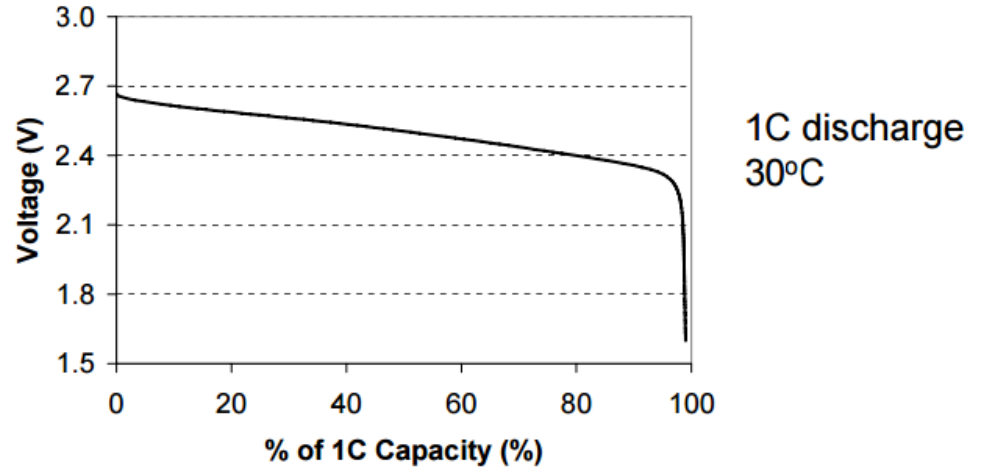
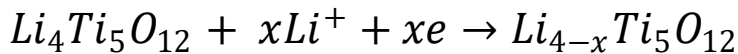


LITHIUM BATTERY FOR SUSTAINABLE ENERGY STORAGE

Positive Active Material (LMO):

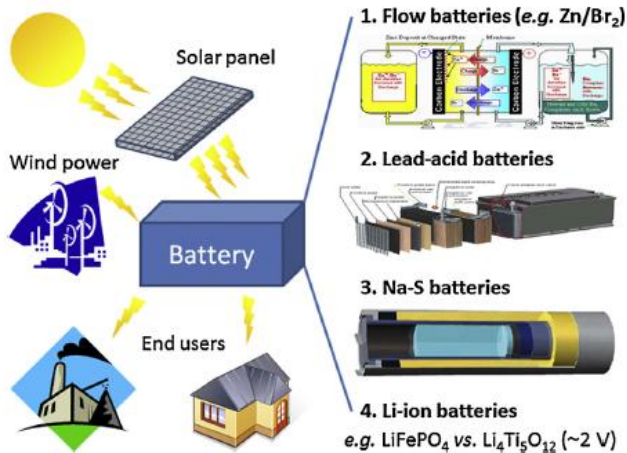


Negative Active Material (LTO):



$$E_{\text{cell}} = 2.5 \text{ V}$$

20.000 ciclos de carga y descarga
Vida útil de paneles solares, mas
20 años.



LTO/LMO battery

Much higher available energy and voltage than Ni-MHO

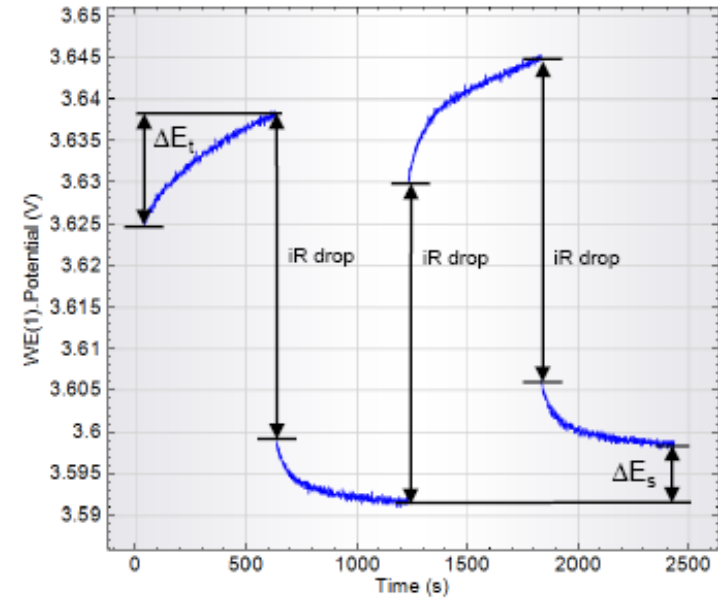
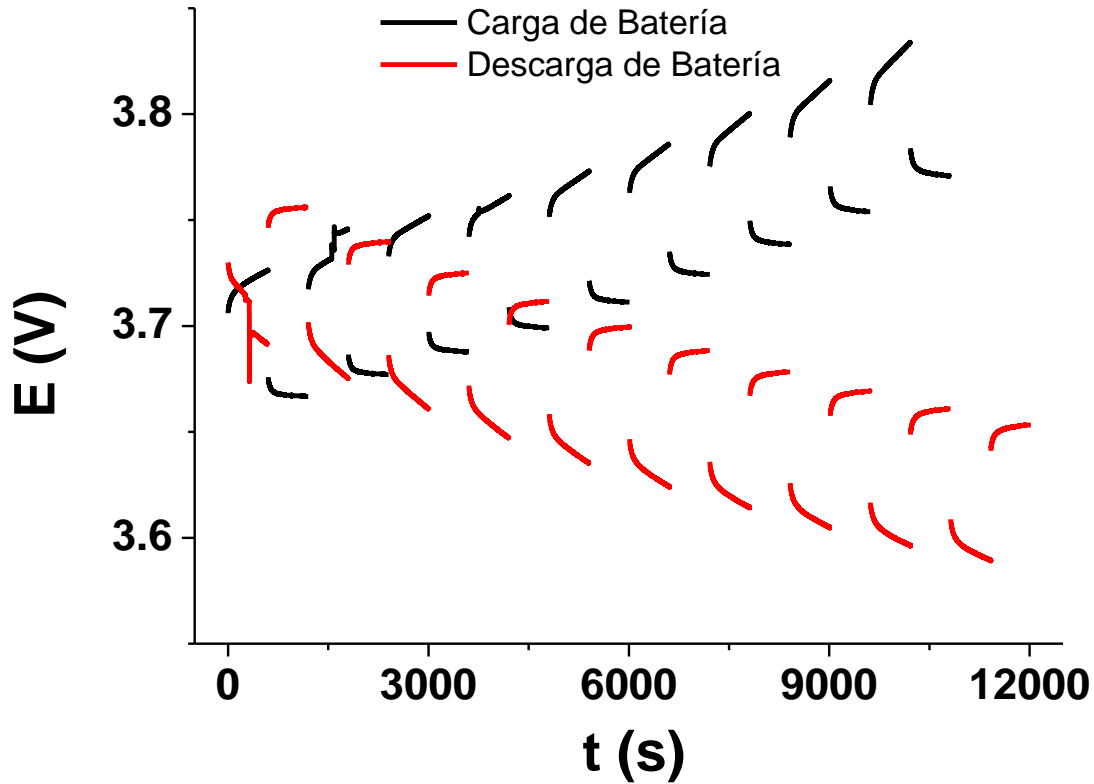
- **Advantages LTO**

- High Power, less impedance than graphite
- Outstanding Safety
- No SEI layer. No lithium dendrites
- Remote risk of thermal runaway
- Stable active materials
- Long Life
- Zero strain material (LTO ~ 0.2 % volume change) vs. Graphite ~ 9% volume change)
- Low temperature performance
- More electrolyte choices
- Disadvantages
- Lower Energy Density [?](#)
- Low Cell Voltage. (1.5V on negative)

- **Advantages LMO**

- High Voltage
- High voltage profile to couple with lithium titanate
- Low Cost Low LMO (3/4 of LiFePO_4 , 1/2 of LiNiCo Oxide, 1/3 of LiCoO_2).
- Power Capability
- Outstanding Safety
- O_2 under high temperature.

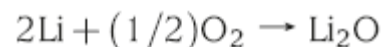
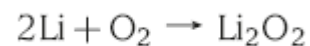
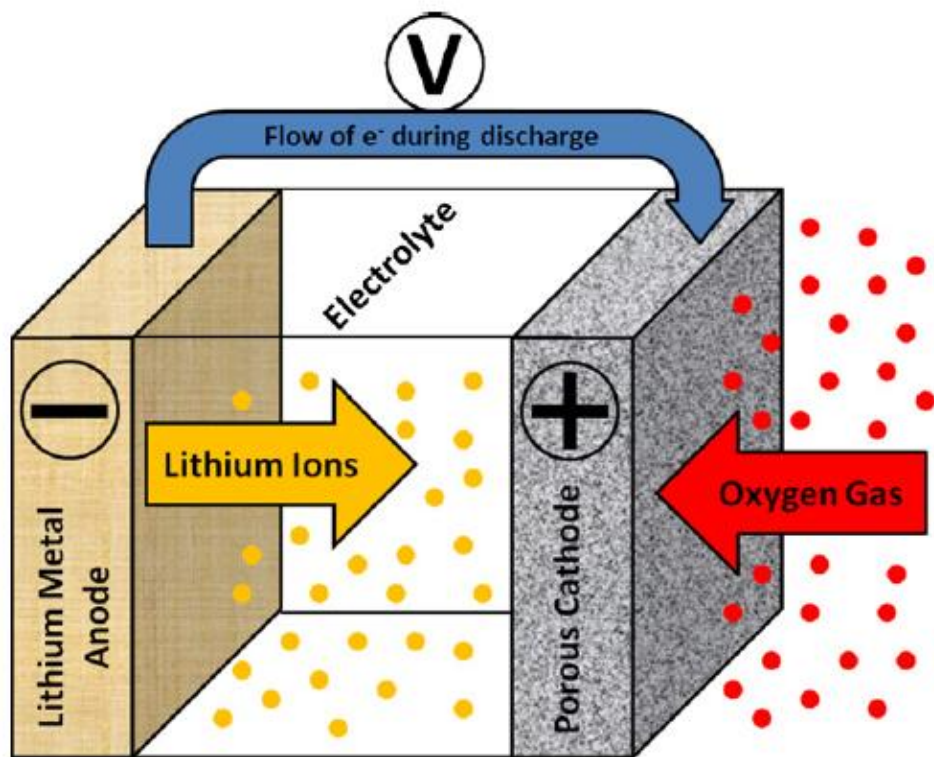
Aplicación de Técnica GITT a una batería 18650 de Li ion de 2,4 Ah descargando a C/10 o sea con pulsos de corriente de 240 mA



$$D = \frac{4}{\pi} \left(\frac{iV_m}{z_A F S} \right)^2 \left[\frac{(dE/d\delta)}{(dE/d\sqrt{t})} \right]^2$$

$$D = \frac{4}{\pi \tau} \left(\frac{n_m V_m}{S} \right)^2 \left(\frac{\Delta E_s}{\Delta E_t} \right)^2$$

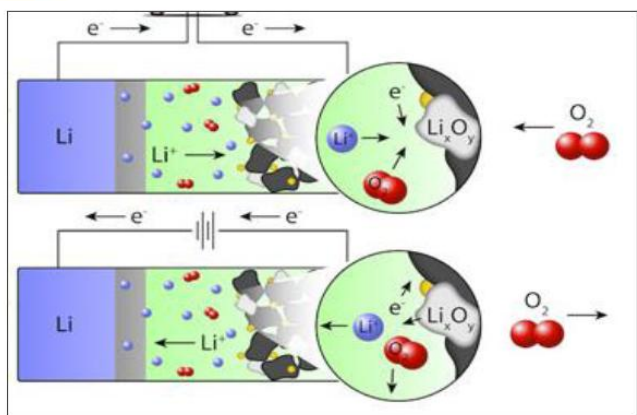
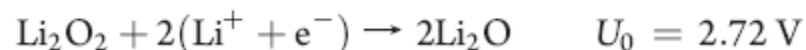
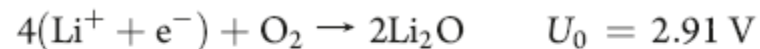
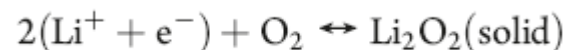
Rechargeable Li Air Battery

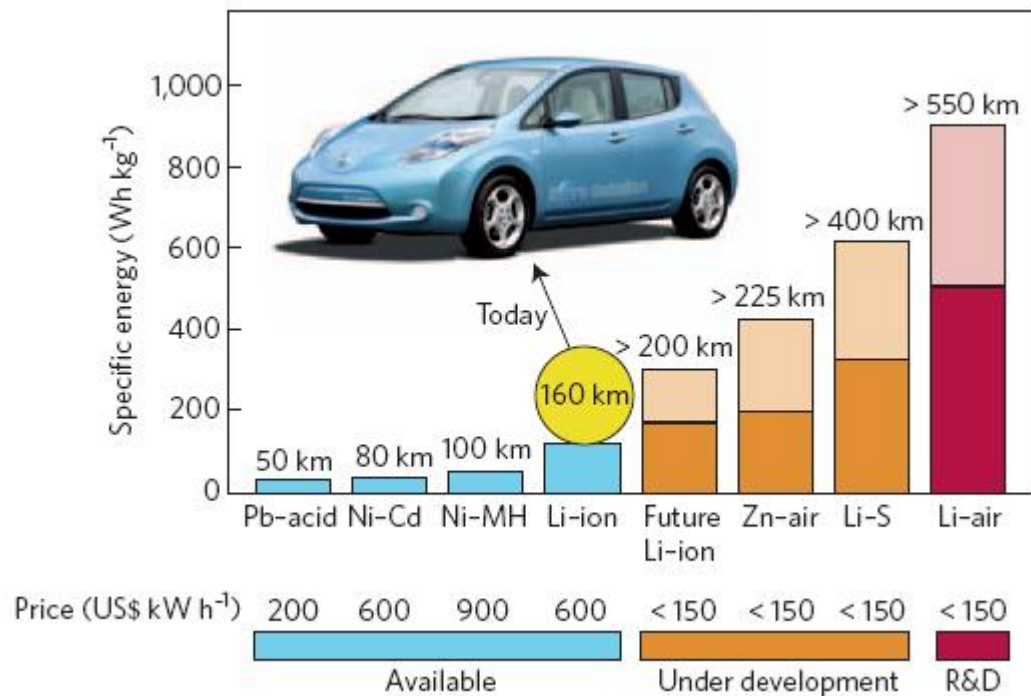


Lithium Anode



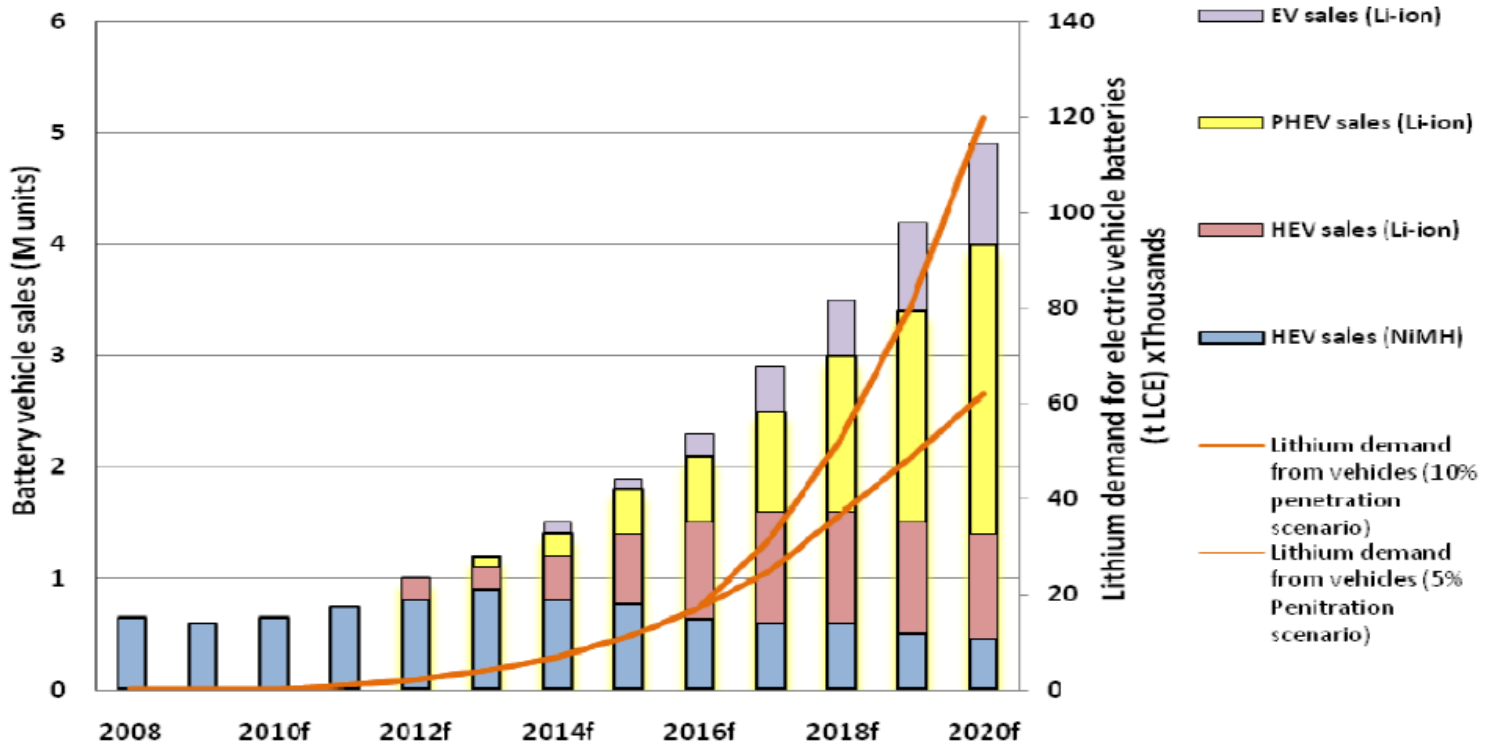
Carbon Cathode





Battery	Cell voltage (V)	Theoretical specific energy (Wh kg ⁻¹)	Theoretical energy density (Wh l ⁻¹)
Today's Li-ion $\frac{1}{2}C_6Li + Li_{0.5}CoO_2 \leftrightarrow 3C + LiCoO_2$	3.8	387	1,015
Zn-air $Zn + \frac{1}{2}O_2 \leftrightarrow ZnO$	1.65	1,086	6,091* (ZnO)
Li-S $2Li + S \leftrightarrow Li_2S$	2.2	2,567	2,199† (Li + Li ₂ S)
Li-O ₂ (non-aqueous) $2Li + O_2 \leftrightarrow Li_2O_2$	3.0	3,505	3,436‡ (Li + Li ₂ O ₂)
Li-O ₂ (aqueous) $2Li + \frac{1}{2}O_2 + H_2O \leftrightarrow 2LiOH^§$	3.2	3,582	2,234 (Li + H ₂ O + LiOH)

Proyección de ventas de automóviles eléctricos



Fuente: Roskill

LITHIUM–AIR AND OTHER BATTERIES BEYOND LITHIUM-ION BATTERIES

K. M. Abraham

1	INTRODUCTION	161
2	ULTRAHIGH-ENERGY-DENSITY BATTERIES	163
3	RECHARGEABLE LITHIUM–AIR BATTERIES	165
3.1	NONAQUEOUS LITHIUM–AIR BATTERY	167
3.2	OXYGEN REDUCTION REACTIONS IN ORGANIC ELECTROLYTES FOR THE LITHIUM–AIR BATTERY	169
3.3	OXYGEN REDUCTION REACTIONS IN IONIC LIQUID ELECTROLYTES FOR THE LITHIUM–AIR BATTERY	173
4	LITHIUM–AIR CELLS	178
4.1	CATALYSIS OF THE LITHIUM–AIR BATTERY	183
4.2	LITHIUM ANODE PROTECTION	185
5	SOLID-STATE LITHIUM–AIR BATTERIES	186
6	PERSPECTIVE	188

1 INTRODUCTION

The nonaqueous lithium–air battery, comprised of a lithium-metal anode and an oxygen cathode, is the highest-energy-density battery that can be developed into a practical system. It promises to overcome the energy density limitations of lithium-ion batteries, which have played an unequalled part in the modern electronic technology revolution. Lithium-ion batteries are indispensable in our everyday life as power sources for wireless telephones, laptop and tablet computers, music players, digital cameras, and many other consumer devices. The discovery of high-energy-density (energy stored per unit mass and volume) battery chemical couples based on Li intercalating negative and positive electrodes together with chemically and electrochemically compatible nonaqueous electrolytes, and engineering of the resulting Li-ion

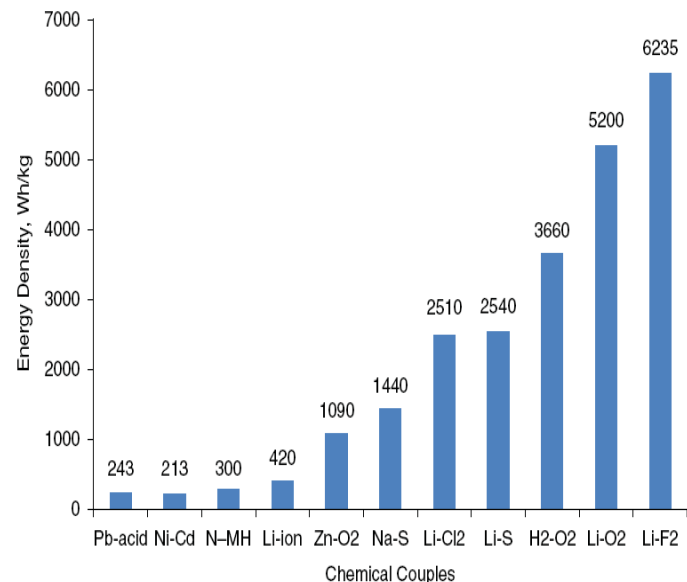


TABLE 1 Theoretical Voltages and Specific Energies of Metal–Air Batteries

Metal–air battery	Calculated OCV (V)	Theoretical specific energy (Wh/kg)	
		Including oxygen	Excluding oxygen
Li–O ₂	2.91	5,200	11,140
Na–O ₂	1.94	1,677	2,260
Ca–O ₂	3.12	2,990	4,180
Mg–O ₂	2.93	2,789	6,462
Zn–O ₂	1.65	1,090	1,350

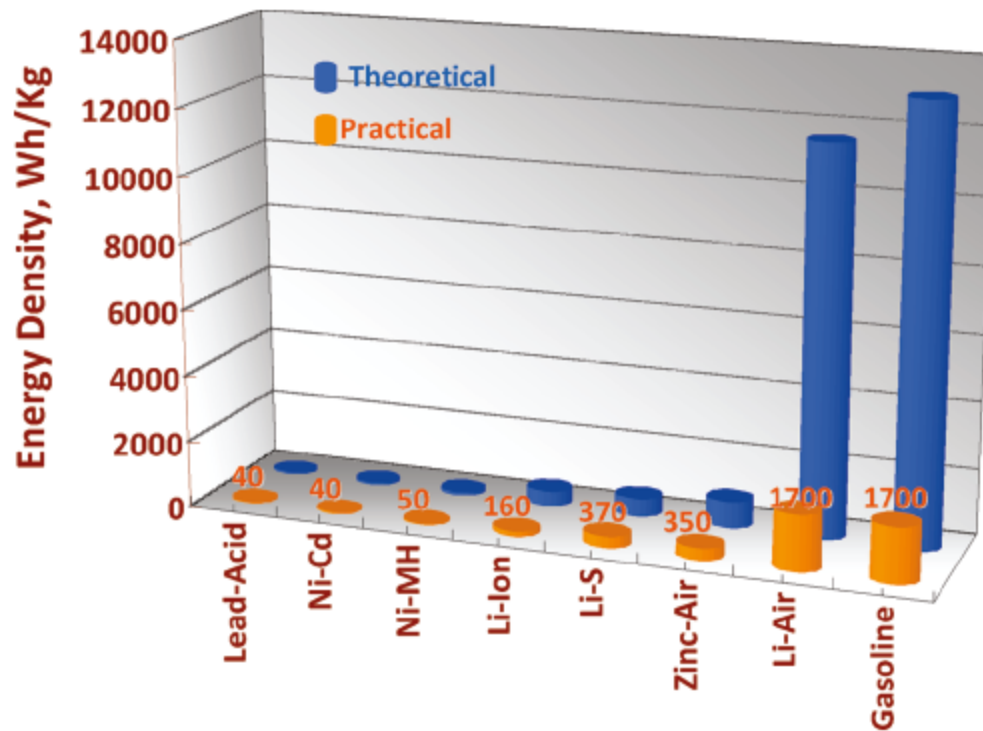


Figure 1. The gravimetric energy densities (Wh/kg) for various types of rechargeable batteries compared to gasoline. The theoretical density is based strictly on thermodynamics and is shown as the blue bars while the practical achievable density is indicated by the orange bars and numerical values. For Li-air, the practical value is just an estimate. For gasoline, the practical value includes the average tank-to-wheel efficiency of cars.

Representacion esquematica de celdas de:

ion-litio,

Li-O₂ no acuosa,

Li-O₂ acuosa,

Li-S

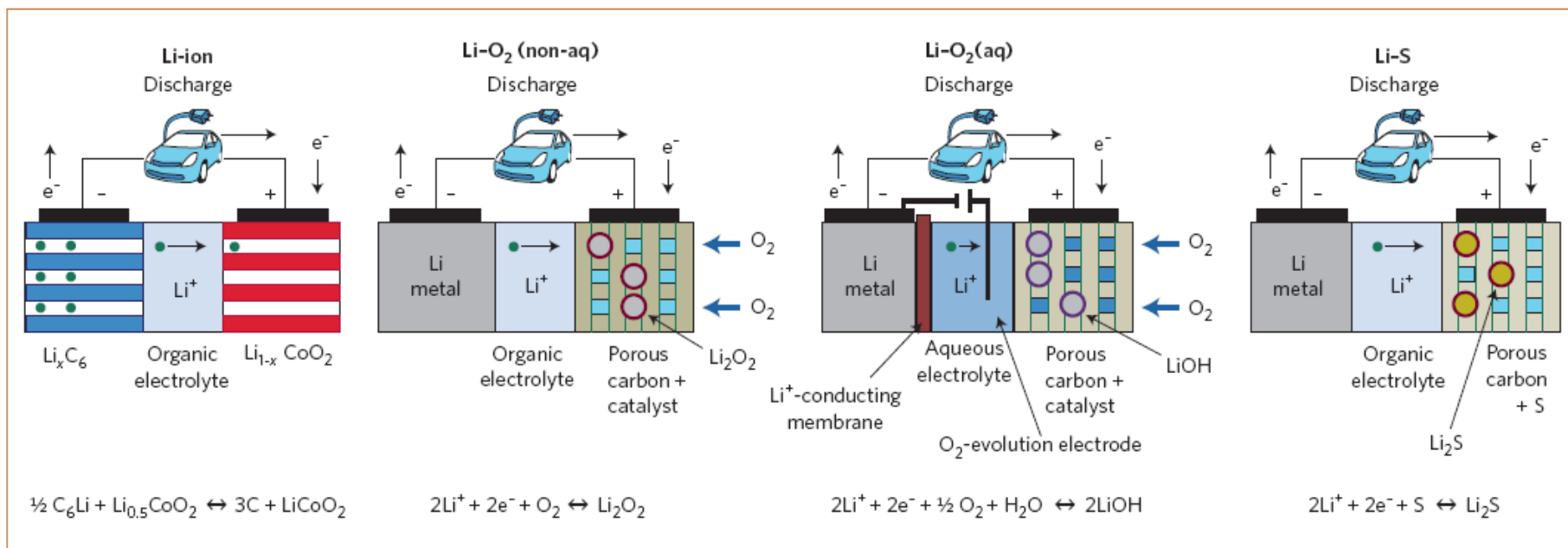
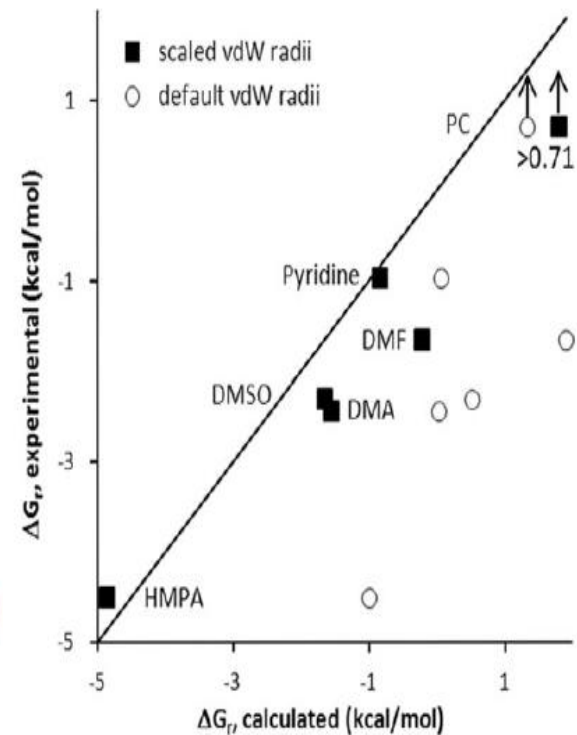
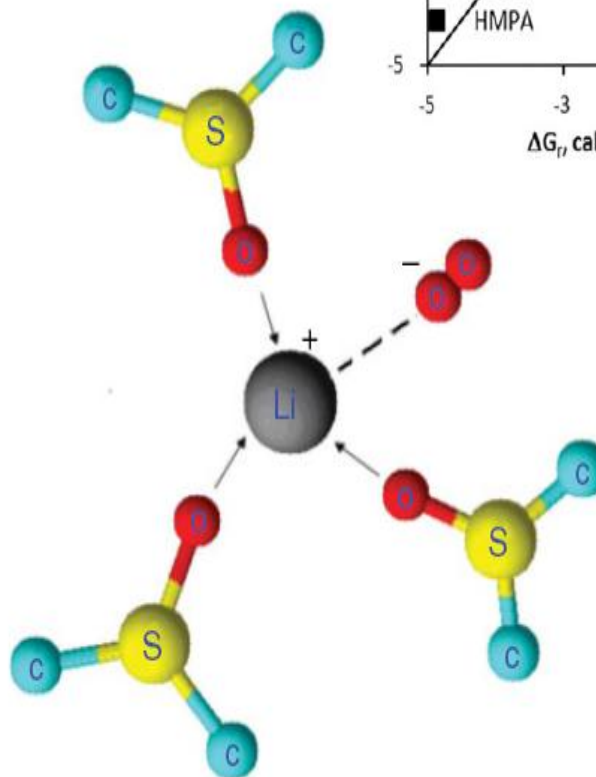
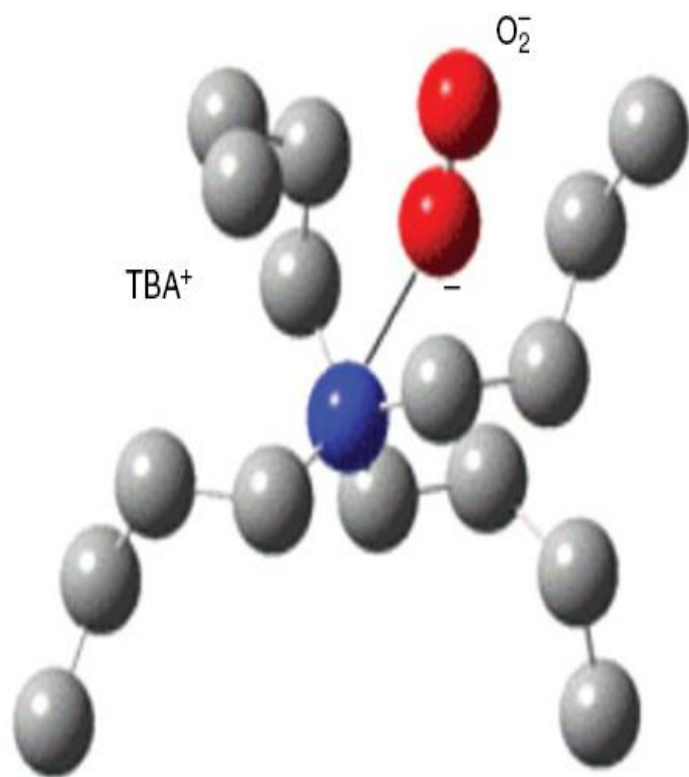
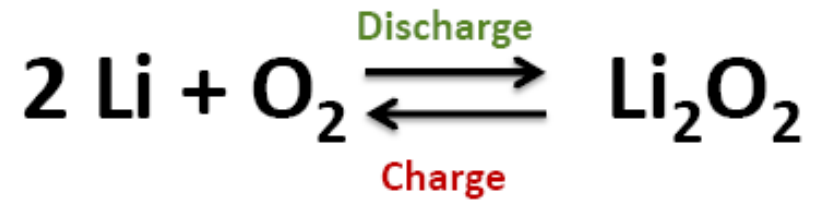
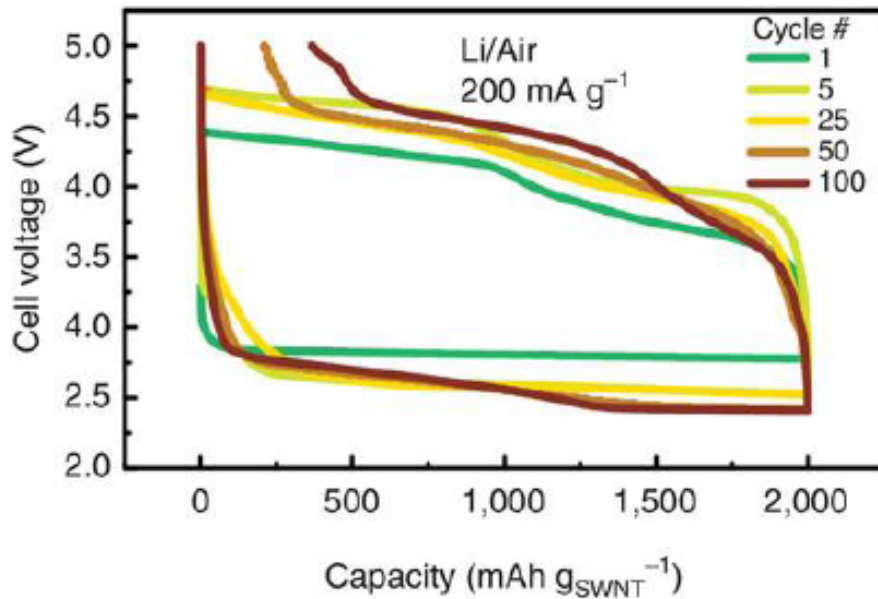


TABLE 2 Solvent Properties

Solvent	ϵ 25°C	DN (kcal/mol)	Viscosity, η (cP)	Oxygen solubility (mM/cm ³)
Dimethyl sulfoxide	48.01	29.8	1.94	2.10
Acetonitrile	36.64	14.1	0.36	8.10
Tetraethylene glycol dimethyl ether	7.79	16.6	4.05	4.43
1,2-dimethoxyethane	7.20	20.0	0.46	9.57
Propylene carbonate	64.4	15.1	2.53	
Ethylene carbonate	89.6	16.4	1.85	1.55



High recharge overpotential and capacity fading upon cycling



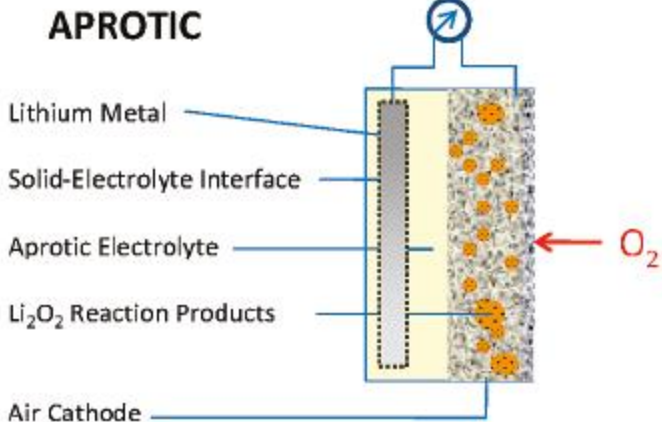
Side reactions

Side products

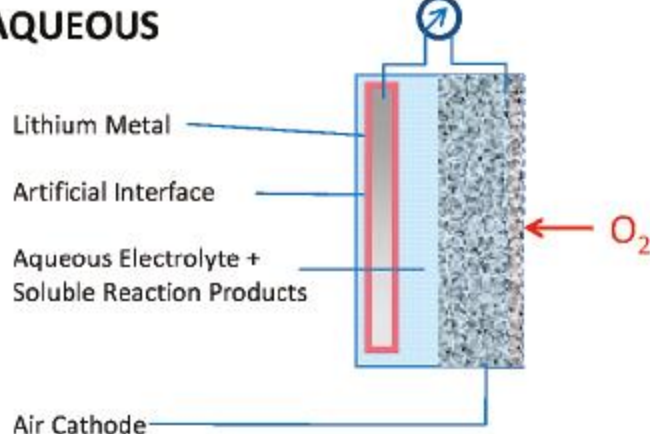
Loss of capacity

Distintas configuraciones de baterías de Li-aire

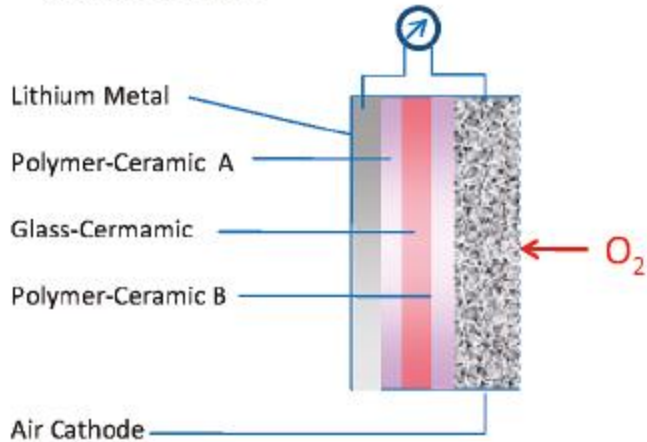
APROTIC



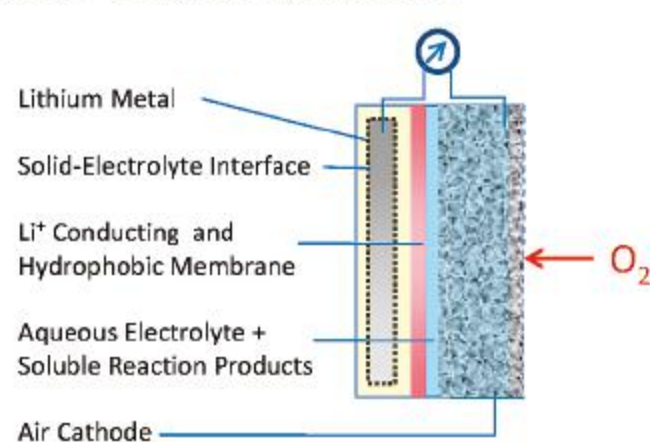
AQUEOUS



SOLID STATE



MIXED AQUEOUS/APROTIC



Ciclos de Carga-Descarga

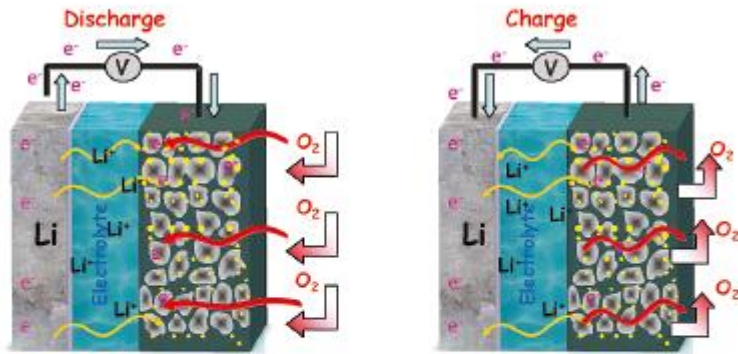
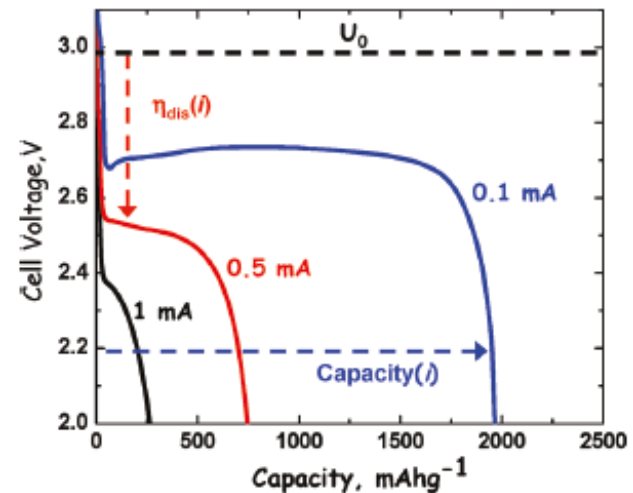
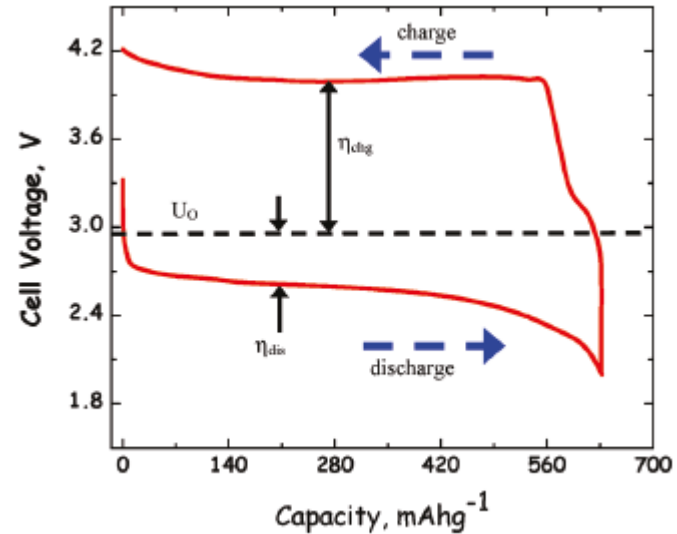
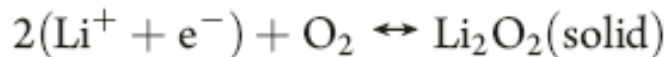
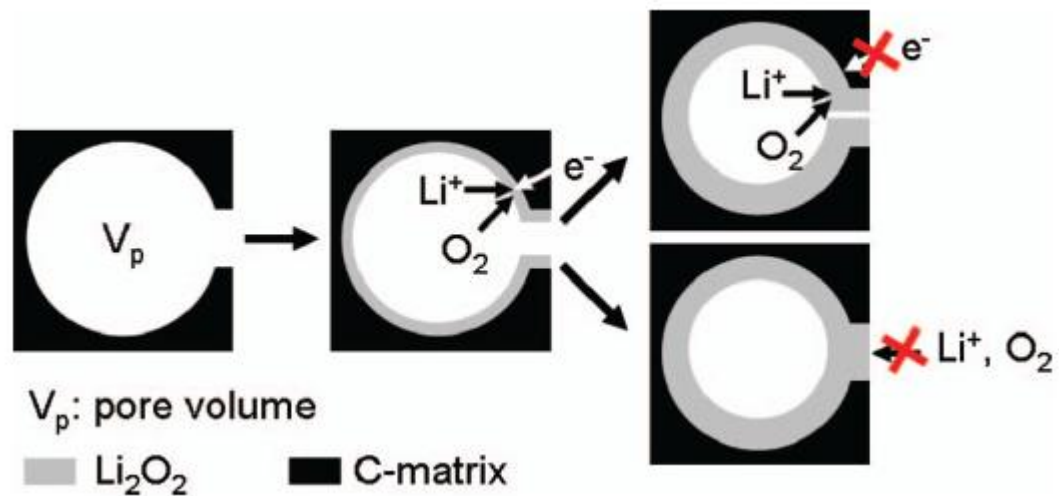
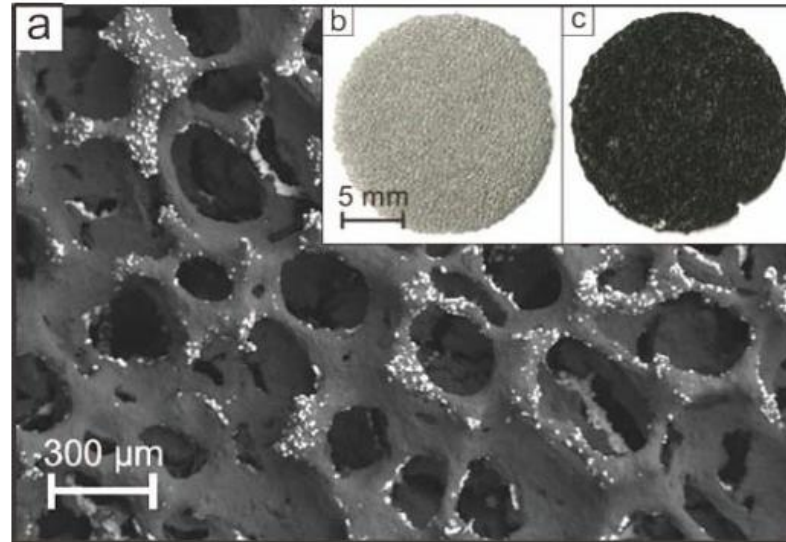


Figure 4. Schematic operation proposed for the rechargeable aprotic Li-air battery. During discharge, the spontaneous electrochemical reaction $2\text{Li} + \text{O}_2 \rightarrow \text{Li}_2\text{O}_2$ generates a voltage of 2.96 V at equilibrium (but practically somewhat less due to overpotentials). During charge, an applied voltage larger than 2.96 V (~ 4 V is required due to overpotentials) drives the reverse electrochemical reaction $\text{Li}_2\text{O}_2 \rightarrow 2\text{Li} + \text{O}_2$.



ESTRUCTURA POROSA DEL CATODO DE CARBON



DESAFIOS TECNOLOGICOS

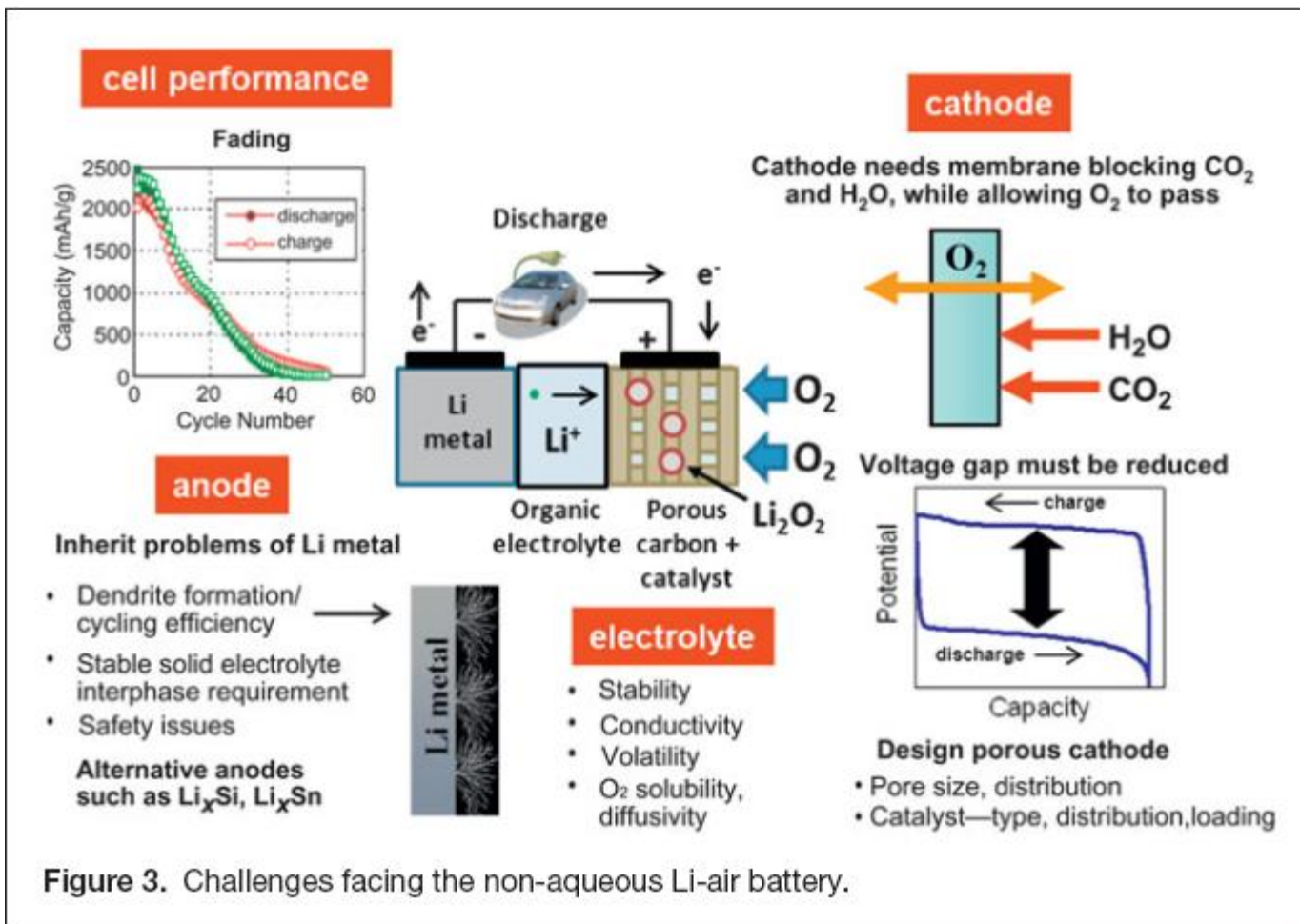


Figure 3. Challenges facing the non-aqueous Li-air battery.

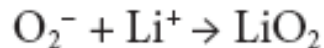
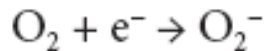
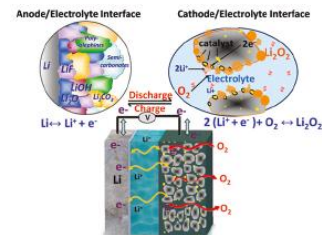
Desafíos

- Baterías de Li-aire tienen mayor densidad gravimétrica de energía que LiCoO_2 (130 mAh.g^{-1}).
- Comprender las reacciones electroquímicas de carga-descarga.
- Desarrollar electrolitos resistentes a la oxidación en presencia de O_2 y Li_2O_2 .
- Entender la naturaleza de electrocatálisis con la formación de productos insolubles (Li_2O_2).
- Desarrollar nuevas nanoestructuras de cátodos de aire para facilitar el transporte de O_2 y Li^+ .
- Mejorar las condiciones de ánodos de litio metálico para ciclos repetidos sin dendritas.
- Desarrollo de membranas permeables a O_2 del aire filtrando H_2O y CO_2 .

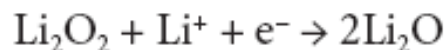
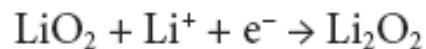
Lithium–Air Battery: Promise and Challenges

G. Girishkumar,* B. McCloskey, A. C. Luntz, S. Swanson, and W. Wilcke

IBM Research - Almaden, 650 Harry Road, San José, California 95120



Reducción electroquímica



Re oxidación del peróxido

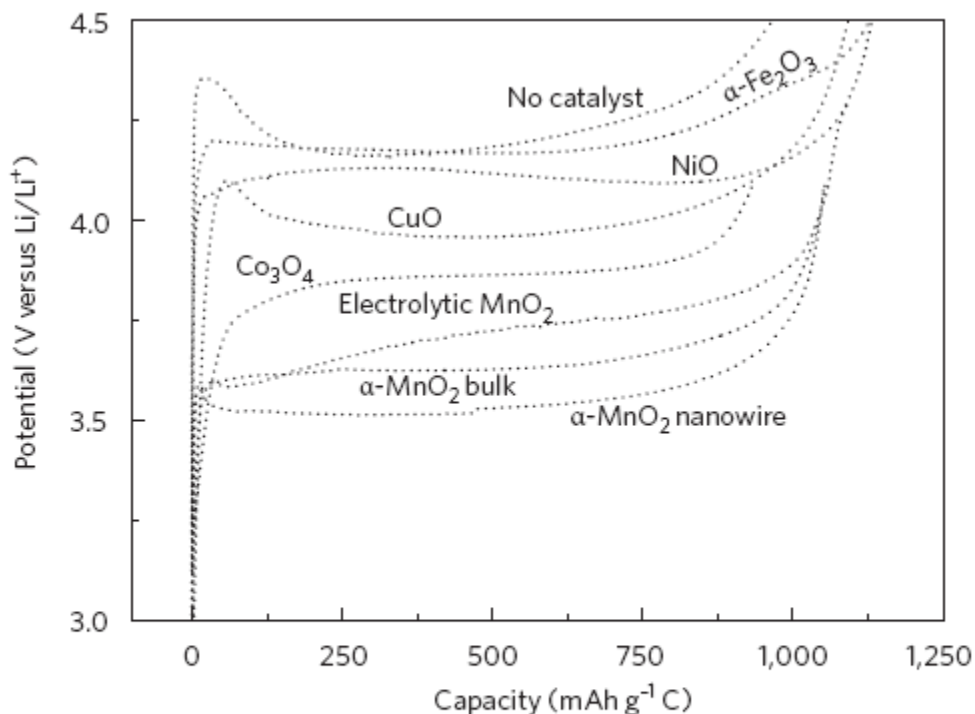
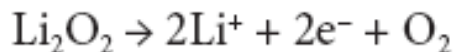
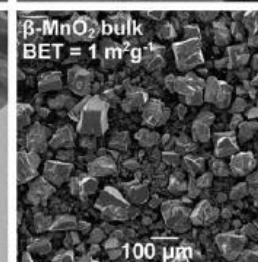
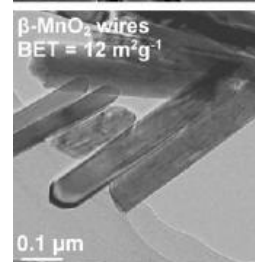
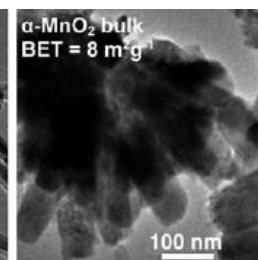
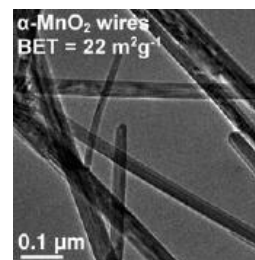
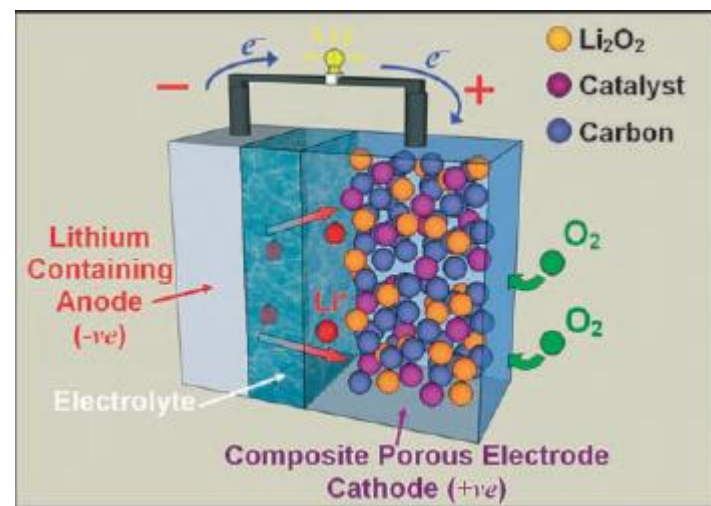
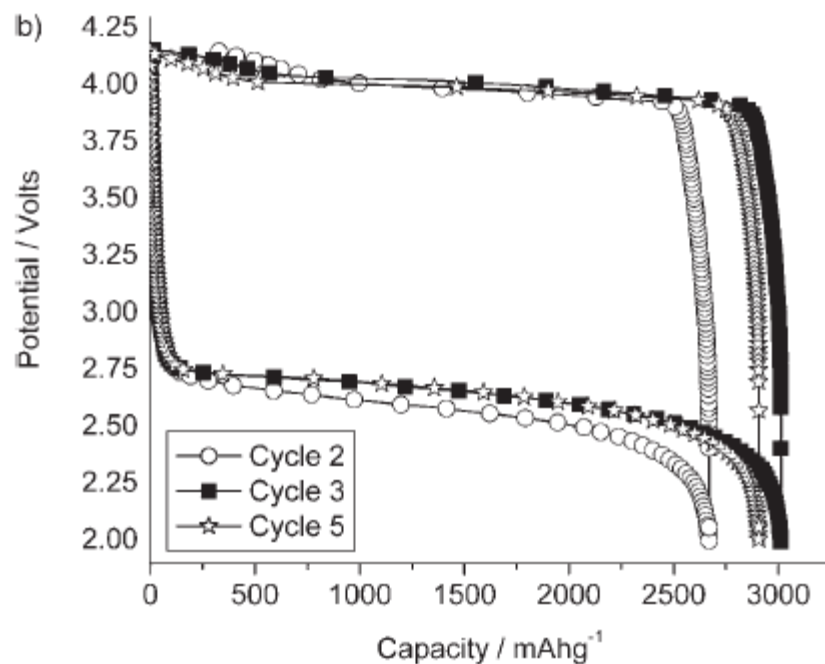


Figure 4 | First galvanostatic charge, $i = 70 \text{ mA g}^{-1} \text{ C}$ (that is, Li₂O₂ oxidation) for various catalyst-containing Li-O₂ cells in this study⁷⁷. Figure adapted with permission from ref. 77, © 2010 ECS.

α -MnO₂ Nanowires: A Catalyst for the O₂ Electrode in Rechargeable Lithium Batteries**

Aurélie Débart, Allan J. Paterson, Jianli Bao, and Peter G. Bruce*

Angew. Chem. Int. Ed. 2008, 47, 4521–4524



Platinum–Gold Nanoparticles: A Highly Active Bifunctional Electrocatalyst for Rechargeable Lithium–Air Batteries

Yi-Chun Lu,[†] Zhichuan Xu,[†] Hubert A. Gasteiger,^{†,§} Shuo Chen,[†] Kimberly Hamad-Schifferli,[†] and Yang Shao-Horn^{*,†}

Departments of Materials Science and Engineering, Mechanical Engineering, and Biological Engineering, Massachusetts Institute of Technology, Cambridge, Massachusetts 02139

J. AM. CHEM. SOC. 2010, 132, 12170–12171

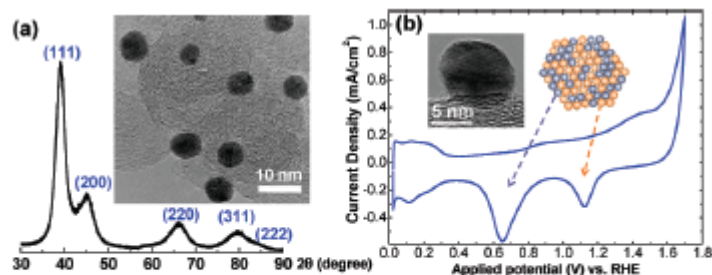


Figure 1. (a) Representative TEM image (top right) and XRD data of PtAu/C. (b) Cyclic voltammograms of PtAu/C collected in Ar-saturated 0.5 M H₂SO₄ between 0.05 and 1.7 V vs RHE (room temperature and 50 mV/s). Insets: (left) HRTEM image of PtAu/C and (right) schematic representation of PtAu, with arrows indicating the CV signatures for Pt (gray) and Au (yellow).

